Intracellular Angiotensin-II Interacts With Nuclear Angiotensin Receptors in Cardiac Fibroblasts and Regulates RNA Synthesis, Cell Proliferation, and Collagen Secretion

Artavazd Tadevosyan, Jiening Xiao, Sirirat Surinkaew, Patrice Naud, Clémence Merlen, Masahide Harada, Xiaoyan Qi, David Chatenet, Alain Fournier, Bruce G. Allen, et al.

▶ **To cite this version:**

Artavazd Tadevosyan, Jiening Xiao, Sirirat Surinkaew, Patrice Naud, Clémence Merlen, et al.. Intracellular Angiotensin-II Interacts With Nuclear Angiotensin Receptors in Cardiac Fibroblasts and Regulates RNA Synthesis, Cell Proliferation, and Collagen Secretion. Journal of the American Heart Association, 2017, 6 (4), pp.e004965. 10.1161/jaha.116.004965 . pasteur-01533741

HAL Id: pasteur-01533741
https://riip.hal.science/pasteur-01533741

Submitted on 6 Jun 2017

HAL is a multi-disciplinary open access archive for the deposit and dissemination of scientific research documents, whether they are published or not. The documents may come from teaching and research institutions in France or abroad, or from public or private research centers.

L'archive ouverte pluridisciplinaire **HAL**, est destinée au dépôt et à la diffusion de documents scientifiques de niveau recherche, publiés ou non, émanant des établissements d'enseignement et de recherche français ou étrangers, des laboratoires publics ou privés.

Distributed under a Creative Commons Attribution - NonCommercial - NoDerivatives 4.0 International License

ORIGINAL RESEARCH

American Heart Association | American Stroke Association

Intracellular Angiotensin-II Interacts With Nuclear Angiotensin Receptors in Cardiac Fibroblasts and Regulates RNA Synthesis, Cell Proliferation, and Collagen Secretion

Artavazd Tadevosyan, PhD; Jiening Xiao, PhD; Sirirat Surinkaew, PhD; Patrice Naud, PhD; Clémence Merlen, PhD; Masahide Harada, MD, PhD; Xiaoyan Qi, PhD; David Chatenet, PhD; Alain Fournier, PhD; Bruce G. Allen, PhD; Stanley Nattel, MD

***Background*—**Cardiac fibroblasts play important functional and pathophysiological roles. Intracellular ("intracrine") angiotensin-II (Ang-II) signaling regulates intercellular communication, excitability, and gene expression in cardiomyocytes; however, the existence and role of intracrine Ang-II signaling in cardiac fibroblasts is unstudied. Here, we evaluated the localization of Ang-II receptors on atrial fibroblast nuclei and associated intracrine effects of potential functional significance.

***Methods and Results*—**Immunoblots of subcellular protein-fractions from isolated canine atrial fibroblasts indicated the presence of nuclear Ang-II type 1 receptors (AT1Rs) and Ang-II type 2 receptors (AT2Rs). Fluorescein isothiocyanate–Ang-II binding displaceable by AT1R- and AT2R-blockers was present on isolated fibroblast nuclei. G-protein subunits, including Gαq/11, Gαi/3, and Gβ, were observed in purified fibroblast nuclear fractions by immunoblotting and intact-fibroblast nuclei by confocal immunocytofluorescence microscopy. Nuclear AT1Rs and AT2Rs regulated de novo RNA synthesis ([α^{32}P]UTP incorporation) via IP3R- and NO-dependent pathways, respectively. In intact cultured fibroblasts, intracellular Ang-II release by photolysis of a membrane-permeable caged Ang-II analog led to IP3R-dependent nucleoplasmic Ca^{2+}-liberation, with IP3R3 being the predominant nuclear isoform. Intracellular Ang-II regulated fibroblast proliferation ([^{3}H]thymidine incorporation), collagen-1A1 mRNA-expression, and collagen secretion. Intracellular Ang-II and nuclear AT1R protein levels were significantly increased in a heart failure model in which atrial fibrosis underlies atrial fibrillation.

***Conclusions*—**Fibroblast nuclei possess AT1R and AT2R binding sites that are coupled to intranuclear Ca^{2+}-mobilization and NO liberation, respectively. Intracellular Ang-II signaling regulates fibroblast proliferation, collagen gene expression, and collagen secretion. Heart failure upregulates Ang-II intracrine signaling-components in atrial fibroblasts. These results show for the first time that nuclear angiotensin-II receptor activation and intracrine Ang-II signaling control fibroblast function and may have pathophysiological significance. **(*J Am Heart Assoc*. 2017;6:e004965. DOI: 10.1161/JAHA.116.004965.)**

Key Words: atrial fibrillation • fibroblasts • intracrine angiotensin system • nuclear receptors • remodeling

Downloaded from http://jaha.ahajournals.org/ by guest on July 17, 2017

Cardiac fibroblasts play a fundamental role in regulating the structural, mechanical, and electrical properties of the heart.[1,2] Fibroblast proliferation and differentiation to activated myofibroblasts cause increased extracellular-matrix protein synthesis, tissue fibrosis, and electrophysiological disturbances/arrhythmias.[1,2] The functional properties and behavior of cardiac fibroblasts are controlled by a variety of proinflammatory cytokines, vasoactive peptides, and hormones.[3] Atrial fibrillation (AF) is the most common cardiac arrhythmia in clinical practice, is often

From the Department of Medicine and Research Center, Montreal Heart Institute and Université de Montréal, Quebec, Canada (A.T., J.X., S.S., P.N., C.M., X.Q., B.G.A., S.N.); Department of Biochemistry and Molecular Medicine, Université de Montréal, Quebec, Canada (B.G.A.); Institut National de la Recherche Scientifique-Institut Armand Frappier, Laval, Québec, Canada (D.C., A.F.); Department of Cardiology, Fujita Health University School of Medicine, Toyoake, Japan (M.H.); Department of Pharmacology and Therapeutics, McGill University, Montréal, Quebec, Canada (B.G.A., S.N.); Institute of Pharmacology, West German Heart and Vascular Center, University Duisburg-Essen, Duisburg, Germany (S.N.).

Accompanying Figures S1 through S4 are available at http://jaha.ahajournals.org/content/6/4/e004965/DC1/embed/inline-supplementary-material-1.pdf

Correspondence to: Stanley Nattel, MD, or Bruce G. Allen, PhD, 5000 Belanger St, Montreal, Quebec, Canada H1T 1C8. E-mails: stanley.nattel@icm-mhi.org, bruce.g.allen@umontreal.ca

Received January 9, 2017; accepted February 16, 2017.

© 2017 The Authors. Published on behalf of the American Heart Association, Inc., by Wiley. This is an open access article under the terms of the Creative Commons Attribution-NonCommercial-NoDerivs License, which permits use and distribution in any medium, provided the original work is properly cited, the use is non-commercial and no modifications or adaptations are made.

a major therapeutic challenge, and in many clinical and experimental AF paradigms fibroblast activation and tissue fibrosis play central roles.[3]

The renin–angiotensin system, operating predominantly through angiotensin-II (Ang-II), is a major regulator of fibroblast homeostasis.[4] Ang-II leads to dose-dependent collagen production within the myocardium and has emerged as a key mediator of myocardial fibrosis.[5] The classical notion of the renin–angiotensin system was of an endocrine system in which the octapeptide Ang-II is delivered systemically to target cells. Evidence is accumulating that, along with traditional circulating Ang-II delivery, cardiac cells are able to synthesize biologically active Ang-II intracellularly.[6] In fibroblasts exposed to isoproterenol or high glucose concentrations, intracellular Ang-II levels are increased.[7] Similarly, isolated cardiomyocytes from diabetic rats have higher Ang-II concentrations compared to healthy animals.[8] Intracellular microinjection of Ang-II into cardiomyocytes alters cardiac physiological properties such as cell volume, cell communication, and ion-channel function.[9] Ang-II type 1 (AT1Rs) and type 2 receptors (AT2Rs) are located on cardiomyocyte nuclei and control gene expression[9]; however, whether fibroblasts possess functionally relevant nuclear receptors remains untested. Here, we addressed the nuclear expression of AT1Rs and AT2Rs in atrial fibroblasts, examined their coupling to signaling systems and functional properties, and examined whether atrial-fibroblast nuclear ATRs are altered in congestive heart failure (CHF). To directly study intracrine signaling, we exploited a novel photoreleasable caged-Ang-II derivative, [Tyr(DMNB)^4]Ang-II.[10–12]

Materials and Methods

All animal protocols in this study were approved by the institutional ethics committee for animal research and were in accordance with the guidelines of the National Institutes of Health. A total of 74 control dogs and 6 CHF dogs were used for fibroblast isolation and study.

Atrial fibroblasts were freshly isolated from canine atria as described below, and were used immediately or with the shortest culture time possible to avoid phenotypic drift. Subcellular fractionation was used to obtain purified membrane, cytosolic, and nuclear preparations for immunoblot determination of ATR localization. Immunocytofluorescence was used to ascertain subcellular protein localization. Standard biochemical assays and specific agonists, antagonists, and blockers were used to determine Ang-II-dependent signaling mechanisms and responses. Selected experiments were performed with focused intracellular release of Ang-II from a caged analog, with appropriate control experiments, to follow the consequences of intracellular Ang-II release. Because of the apparently crucial role of intranuclear Ca^{2+} release via IP3Rs in mediating the effects of nuclear-delimited AT1Rs and the limited specificity of the available pharmacological probe 2-aminoethoxydiphenyl borate (2-APB), we repeated selected experiments with specific siRNA-mediated IP3R knockdown. Finally, selected experiments were performed in fibroblasts isolated from CHF dogs to determine whether this atrial fibrosis–promoting pathology alters the intracrine renin–angiotensin system. Detailed information about specific experiments, reagents, and methods are provided below.

Atrial Fibroblast Isolation

Adult mongrel dogs of either sex (20–30 kg) were anesthetized with morphine (2 mg/kg SC injection) and α-chloralose (120 mg/kg IV), and intravenous heparin (10 000 U) was given. The heart was placed into ice-cold Tyrode solution (136 mmol/L NaCl, 5.4 mmol/L KCl, 1 mmol/L $MgCl_2$ $6H_2O$, 2 mmol/L $CaCl_2$, 0.33 mmol/L NaH_2PO_4 H_2O, 5 mmol/L HEPES, 10 mmol/L glucose, pH 7.4 at room temperature). Following left circumflex coronary artery cannulation and the ligation of all leaks from arterial branches, the atria were perfused for 10 minutes with Ca^{2+}-free Tyrode solution. The atria were digested with 100 U/mL collagenase type II containing 0.1% BSA in Ca^{2+}-free Tyrode. The digested tissue was minced and triturated with a transfer pipette in DMEM. Debris was removed by filtration through a 500-μm nylon mesh and cells were centrifuged at 50*g* for 5 minutes to pellet cardiomyocytes. The supernatant was centrifuged at 850*g* for 15 minutes to pellet fibroblasts. Cells were immediately frozen in liquid nitrogen (freshly isolated cells) or plated in T-75 culture flasks and transferred to an incubator at 5% CO_2/95%-humidified air (37°C) in DMEM supplemented with 10% fetal bovine serum and 2% penicillin/streptomycin. The medium was changed 2 hours after plating to remove dead and nonattached cells and every 24 hours thereafter.

Drugs

The following drugs were used in these experiments: valsartan (a poorly membrane-permeable highly selective AT1R antagonist), PD123177 (a highly selective AT2R antagonist), α-amanitin (an RNA polymerase II inhibitor), L-162,313 (a highly selective AT1R agonist), CGP42112A (a highly selective AT2R agonist), N(G)-nitro-L-arginine methyl ester (L-NAME) (NO inhibitor), and 2-aminoethoxydiphenyl borate (2-APB, IP3R blocker)

Cellular Fractionation and Western Blots

Cardiac fibroblasts were washed in ice-cold PBS: 137 mmol/L NaCl, 2.7 mmol/L KCl, 4.2 mmol/L Na_2HPO_4 H_2O,

Downloaded from http://jaha.ahajournals.org/ by guest on July 17, 2017

1.8 mmol/L KH_2PO_4, pH 7.4 at room temperature. Cells were then placed on an orbital shaker for 20 minutes at 4°C and semipermeabilized in a lysis buffer: 150 mmol/L NaCl, 0.2 mmol/L EDTA, 20 mmol/L HEPES-NaOH, 2 mmol/L dithiothreitol, 2 mmol/L $MgCl_2$, 40 μg/mL digitonin, supplemented with protease/phosphatase inhibitor cocktail just before use. Fibroblasts were then diluted with an equal volume of lysis buffer without digitonin and transferred to a Dounce homogenizer. To further disrupt the cells and free the nuclei, 10 strokes with a tight ("B") pestle were performed. Freshly isolated nuclei were obtained after centrifugation at 850*g* for 15 minutes at 4°C in a swinging-bucket rotor (Sorvall 75-006-434). The supernatants were then transferred to new tubes and further centrifuged at 80 000*g* for 60 minutes at 4°C (Beckman, TLA-100.3 rotor) to separate the nuclear from cytosolic fractions. Figure S1 illustrates the intact nuclei obtained by this method and the high degree of nucleic acid enrichment in the nuclear fraction.

Membrane, cytosolic, or nuclear cell fractions were quantified by Bradford assay, diluted with Laemmli sample buffer, and denatured by heating to 100°C for 5 minutes. Equivalent amounts of protein were separated by SDS-PAGE (7.5–12%) and transferred to polyvinylidene difluoride membranes. Membranes were blocked for 1 hour at room temperature and probed with primary antibodies overnight at 4°C. After extensive washing, membranes were further incubated with secondary antibodies conjugated to horseradish peroxidase and immunoreactive bands detected with enhanced chemiluminescence. After stripping in ReBlot Plus Strong Antibody Stripping Solution, membranes were blocked and reprobed with appropriate primary (AT1R [Alomone Labs], AT2R [Alomone Labs], collagen 1A1 [MD Biosciences], pan-cadherin [Abcam], HSP70 [Cell Signaling Technology], lamin A [Abcam], lamin B [Abcam], lamin A/C [Abcam], endothelial NOS [Abcam], nesprin [ThermoFisher], emerin [Abcam], histone deacetylase-2 [Cell Signaling Technology], vimentin [Santa Cruz Biotechnology], TOPRO-3 [ThermoFisher], Gαq/11 [Santa Cruz Biotechnology], Gαi/3 [Santa Cruz Biotechnology], Gαs [Santa Cruz Biotechnology], Gβ [Santa Cruz Biotechnology], IP3R1 [UC Davis/NIH NeuroMab], IP3R2 [Alomone Labs] and IP3R3 [Novusbio], and secondary antibodies horseradish peroxidase–conjugated anti-mouse or anti-rabbit (Jackson ImmunoResearch Laboratories]).

To assess collagen secretion, 50-μL aliquots of culture media were collected from fibroblasts plated at equal cell density, mixed with Laemmli sample buffer, heated, and loaded on precast 7.5% SDS-PAGE gels. Following migration, proteins were transferred electrophoretically onto nitrocellulose membranes and blocked by incubating with 3% BSA in PBS overnight at 4°C with gentle mixing. Membranes were probed with the primary antibodies for 1 hour at room temperature and then washed and incubated with horseradish peroxidase–conjugated secondary antibodies for an extra 1 hour at room temperature. Signals were detected with enhanced chemiluminescence reagent and band intensities were quantified with Bio-Rad Quantity One software.

Nuclear Fractionation

Freshly isolated nuclei were suspended in 0.25 mol/L sucrose, 50 mmol/L Tris-HCl, 10 mmol/L $MgCl_2$, 1 mmol/L dithiothreitol (pH 7.4) containing protease/phosphatase inhibitor mixture, and incubated for 30 minutes at 4°C with 1% (w/v) sodium citrate. The nuclear suspension was centrifuged for 15 minutes at 500*g* and the supernatant, containing the outer nuclear membrane–enriched fraction, was collected. The remaining pellet was resuspended in 0.3 mol/L sucrose, 50 mmol/L Tris-HCl, 10 mmol/L $MgCl_2$, 1 mmol/L dithiothreitol (pH 7.4) containing DNase (200 μg/mL) and incubated overnight at 4°C on a rotating mixer. The homogenate was centrifuged for 2 hours at 10 000*g* and the supernatant, containing the nucleoplasm, was collected. The pellet, containing the inner nuclear membrane (INM), was purified further on discontinuous sucrose-density gradients (0.25/1.6/2.4 mol/L) centrifuged at 100 000*g* for 20 minutes prior to immunoblotting.

RNA Extraction and Quantitative Polymerase Chain Reaction

Total RNA was extracted with Macherey-Nagel kits. The concentration and purity of the extracted RNA were assessed using a NanoDrop ND-1000 spectrophotometer. Single-stranded cDNA was synthesized from 1 μg of RNA using High Capacity cDNA Reverse Transcription Kits. Quantitative polymerase chain reaction was performed with TaqMan probes and primers on a Stratagene MX3000P system. Samples were assayed in duplicate and normalized to hypoxanthine-guanine phosphoribosyltransferase, an internal housekeeping standard.

IP3R Knockdown

After 1 week in culture, dog fibroblasts were passaged and seeded in 12-well plates. Once 50% to 60% confluence was reached, cells were transfected with siRNA with the use of Lipofectamine RNAiMAX (13778150; Invitrogen). The BLOCK-iT RNAi sequences (Invitrogen) employed were the following: siRNA targeting *ITPR1* gccaagcagtttggcttcatgcaaa; siRNA targeting *ITPR2*: ccgagacttagactttgccaatgat; siRNA targeting *ITPR3*: gccaaccagtgggactacaagaata. Briefly, 100 pmol of siRNA was mixed with 1 μL of lipofectamine in 0.5 mL of antibiotic-free OPTI-MEM medium then added to the well

Downloaded from http://jaha.ahajournals.org/ by guest on July 17, 2017

containing cells in 0.5 mL of antibiotic-free DMEM, mixed gently, and maintained for 24 hours. The medium was replaced with complete medium after 24 hours of transfection. After an additional 24 hours, cells were harvested for further experiments. Knockdown efficiency was assessed for each isoform both by quantitative polymerase chain reaction using specific TaqMan probes and by immunoblotting. $Beta_2$-microglobulin was used as the reference gene.

[^{3}H]Thymidine Incorporation

Cultured atrial fibroblasts were seeded on 24-well plates (30 000 cells/well) and serum-starved for 24 hours. The cells were then treated with various drugs and incubated for an additional 48 hours. DNA synthesis was assessed by adding [^{3}H]thymidine (1 μCi/well) 6 hours prior to the end of the treatment period. Cells were washed twice with ice-cold PBS, suspended in 5% trichloroacetic acid, and incubated for 1 hour at 4°C to precipitate DNA. The trichloroacetic acid was removed and the precipitate was washed with ice-cold PBS followed by 0.5 mol/L NaOH and then resuspended in scintillation fluid. [^{3}H]Thymidine incorporation was determined by liquid scintillation counting.

Transcription Initiation Assays

Freshly isolated fibroblast nuclei were resuspended in 50 mmol/L Tris, 0.15 mol/L KCl, 1 mmol/L $MnCl_2$, 6 mmol/L $MgCl_2$, 1 mmol/L ATP, 2 mmol/L dithiothreitol, 1 U/μL RNase inhibitor, pH 7.9 at room temperature and incubated in the presence of agonist/antagonists and 10 μCi [α^{32}P]UTP (3000 Ci/mmol) at 30°C for 30 minutes. The reaction was terminated upon digestion with DNase and nuclei were lysed with 10 mmol/L Tris–HCl 10 mmol/L EDTA, 1% SDS, pH 8.0 at room temperature. Samples were then transferred onto Whatman GF/C glass microfiber filter discs, washed twice with ice-cold 5% trichloroacetic acid containing 20 mmol/L sodium pyrophosphate, and air dried. Filters were then placed in vials containing scintillation counting liquid and radioactivity reflecting [^{32}P]-incorporation was determined with a beta counter. The DNA content of each sample was measured with a NanoDrop spectrophotometer and [α^{32}P]UTP incorporation was expressed as cpm/ng of DNA.

Immunocytofluorescence

Atrial fibroblasts were plated on 18-mm coverslips and then fixed for 20 minutes with 2% paraformaldehyde in PBS (pH 7.3) at room temperature to preserve cell morphology. The cells were then incubated with a blocking/permeabilizing buffer (PBS, 0.1% Triton X-100, 1% normal donkey serum, 1% BSA) for 1 hour and then incubated overnight at 4°C with the primary antibody diluted in PBS containing 0.05% Triton X-100, 0.5% normal donkey serum, 0.5% BSA. After washing (3×5 minutes) with PBS, cells were incubated in the dark at room temperature for 1 hour, with Alexa-conjugated secondary antibodies diluted in PBS containing 0.05% Triton X-100, 0.5% normal donkey serum, and 0.5% BSA. Cells were then carefully washed (3×5 minutes) with PBS, excess buffer was removed with a tissue, and cells were placed face-down onto microscope slides containing a drop of 1,4-diazabicyclo [2.2.2]octane (DABCO) antiquenching mounting medium (0.2% DABCO in glycerol), and the edges of the coverslip were sealed with nail polish. Images were acquired with an Olympus FluoView FV1000 confocal laser-scanning microscope equipped with a ×40/1.3 oil immersion objective. For multichannel imaging, fluorophores were imaged sequentially. Imaging parameters were adjusted for optimal detection sensitivity with negligible photobleaching.

Fluorometric Nitric Oxide Assay

Isolated nuclei were preincubated with the NO-specific fluorescent indicator, 4,5-diaminofluorescein (DAF-2, 5 μg/mL) in a buffer containing 140 mmol/L NaCl, 14 mmol/L glucose, 4.7 mmol/L KCl, 2.5 mmol/L $CaCl_2$, 1.8 mmol/L $MgSO_4$, 1.8 mmol/L KH_2PO_4, and 0.1 mmol/L L-arginine (pH 7.4) for 30 minutes at 37°C. Nuclei were washed 3 times with HEPES buffer (20 mmol/L HEPES, 115 mmol/L NaCl, 5.4 mmol/L KCl, 1.8 mmol/L $CaCl_2$, 0.8 mmol/L $MgCl_2$, 13.8 mmol/L glucose, pH 7.4) to remove any unbound DAF-2 and then incubated with various agonists/antagonists at 37°C. Samples were transferred to a 96-well microplate and DAF fluorescence was measured using a BioTek Synergy 2 Microplate Reader (excitation λ=488 nm, emission λ=510 nm).

[Tyr(DMNB)^4]Ang-II Uncaging and Intracellular Ca^{2+} Measurement

To monitor changes in intracellular Ca^{2+} concentrations, freshly isolated fibroblasts, seeded in FluoroDishes, were loaded with 5 μmol/L Fluo-4AM in DMEM in the presence or absence of [Tyr(DMNB)^4]Ang-II and placed into an incubator for 30 minutes at 37°C. Cells were washed 3 times with indicator-free medium and incubated for an additional 15 minutes to allow complete de-esterification. DRAQ5, a membrane-permeable fluorescent dye with high affinity for double-stranded DNA, was used to stain the nucleus and to focus the UV-laser into a rectangular region on the nucleus. Images were acquired with a Zeiss LSM 7 Duo microscope (combined LSM 710 and Zeiss Live systems) with Zeiss Plan-Apochromat ×63/1.4 oil DIC objective equipped with a BC 405/561 dichroic mirror. Fluo-4AM was excited using an argon laser (488 nm, 100-mW diode) at 1% to 5% laser

Downloaded from http://jaha.ahajournals.org/ by guest on July 17, 2017

intensity and fluorescence emissions between 495 and 550 nm were measured. Cardiac fibroblasts were scanned in bidirectional mode at 30 fps, with pixel size set at 0.2 μm and the pinhole at 1.5 Airy units. After establishing a stable baseline, [Tyr(DMNB)^4]Ang-II was uncaged using a 70-μW pulse of UV light from a 405-nm/30-mW diode. An X-Cite XR2100 optical power measurement system was used to monitor the optical power output at the stage level. Intracellular Ca^{2+} measurements are expressed as a percentage of fluorescence intensity relative to resting fluorescence prior to photolysis ($\Delta[Ca^{2+}]$ $[F/F_0;\%]$).

CHF Model

Adult mongrel dogs were anesthetized with ketamine (5.0 mg/kg IV), diazepam (0.25 mg/kg IV), and halothane (1.5% PI). A unipolar pacing lead was inserted under fluoroscopy into the right ventricular apex from the left internal jugular vein and connected to an electronic pacemaker implanted in a subcutaneous pocket in the neck. After a 24-hour postoperative recovery period, the ventricular pacemaker was programmed to pace the ventricles at 240 bpm for 2 weeks to induce CHF as previously described.[11] Atrial fibrotic remodeling is prominent in the canine CHF model produced by ventricular tachypacing, in which fibrosis plays a fundamental role in the AF substrate.[2,3] Since this model provided the initial basis for the recognition of the importance of atrial fibrosis in AF pathophysiology and has been extensively investigated in our lab,[3] we used it here to address the potential role of changes in intracrine Ang-II signaling in a clinically relevant pathological substrate. Ang-II content was measured by ELISA (Phoenix Pharmaceuticals).

Statistical Analysis

Immunoblot images were acquired from films with a GS-800 2-dimensional scanning system and band intensities were analyzed using Bio-Rad Quantity One software. All N's in the paper are numbers of independent experiments, each from a different heart. Statistical comparisons were performed with *t* tests (when only 2 groups were studied) or 1-way or 2-way ANOVA and Bonferroni post-hoc tests, using GraphPad Prism (Version 5.0 for Windows). All group data are represented as mean±SEM. A 2-tailed $P<0.05$ was considered statistically significant.

Results

Ang-II Receptors Localize to the Nucleus

To assess the subcellular distribution of AT1Rs and AT2Rs, we isolated membrane, cytosolic, and nuclear fractions from atrial cardiac fibroblasts. The purity of the subcellular fractions was validated by immunoblotting for organelle-specific markers including pan-cadherin (membrane), HSP70 (cytosol), and lamin B (nuclei). Immunoblotting with subtype-specific antibodies revealed endogenous AT1R and AT2R immunoreactivity in all 3 fractions but more intense bands were revealed in membrane and nuclear fractions (Figure 1A). To further examine the nuclear compartmentalization of AT1Rs and AT2Rs, we performed a nuclear subfractionation and isolated the outer nuclear membrane, inner nuclear membrane, and nucleoplasm with minimal cross-contamination as defined by nesprin, emerin, and histone deacetylase-2, respectively. In this preparation, AT1R immunoreactivity was detected more prominently on the INM, whereas AT2R immunoreactivity was observed in both the INM and nucleoplasm (Figure 1B). Ang-II binding was examined in intact nuclei using a fluorescently labeled Ang-II analog (fluorescein isothiocyanate–Ang-II) along with the DNA dye DRAQ5. Strong fluorescent labeling was detected, particularly at the nuclear envelope. Fluorescein isothiocyanate–Ang-II (100 nmol/L) binding was displaced (Figure 1C and 1D) by selective extracellular antagonists for both AT1Rs (valsartan, 1 μmol/L) and AT2Rs (PD 123,177, 1 μmol/L). Nuclei preincubated with both valsartan and PD 123,177 showed virtually complete elimination of fluorescein isothiocyanate–Ang-II binding. To further investigate the intracellular distribution of Ang-II receptors, permeabilized atrial fibroblasts were decorated with antibodies to AT1Rs or AT2Rs in addition to the fluorescent nucleic acid stain TOPRO-3 and antibodies against vimentin to delineate the nucleus and cytoskeleton, respectively. Confocal fluorescence microscopy revealed clear nuclear localization for AT1Rs and AT2Rs, with AT1Rs localizing selectively to nuclei (Figure 2). To assess the presence of nuclear heterotrimeric G-proteins potentially coupled to ATRs, we employed immunoblotting and immunofluorescence. Both Gαq/11 and Gαi/3 were present in the nuclear fraction (Figure 3A) and colocalized with TOPRO-3 (Figure 3B). Gαs was only detected in the cytosolic fraction upon immunoblotting, whereas Gβ was present in nuclear fractions. Gαs and Gβ immunofluorescence had a much more diffuse distribution over the cell bodies compared to Gαq/11 and Gαi/3, with some apparent perinuclear localization. Thus, G-protein α- and β-subunits known to mediate AT1R/AT2R effects are present on the nuclei of atrial cardiac fibroblasts.

Nuclear AT1Rs and AT2Rs Are Functional and Regulate Transcription Initiation Through IP3R and NO

To more directly explore the functional consequences of nuclear AT1R/AT2R activation, purified nuclei were incubated

Downloaded from http://jaha.ahajournals.org/ by guest on July 17, 2017

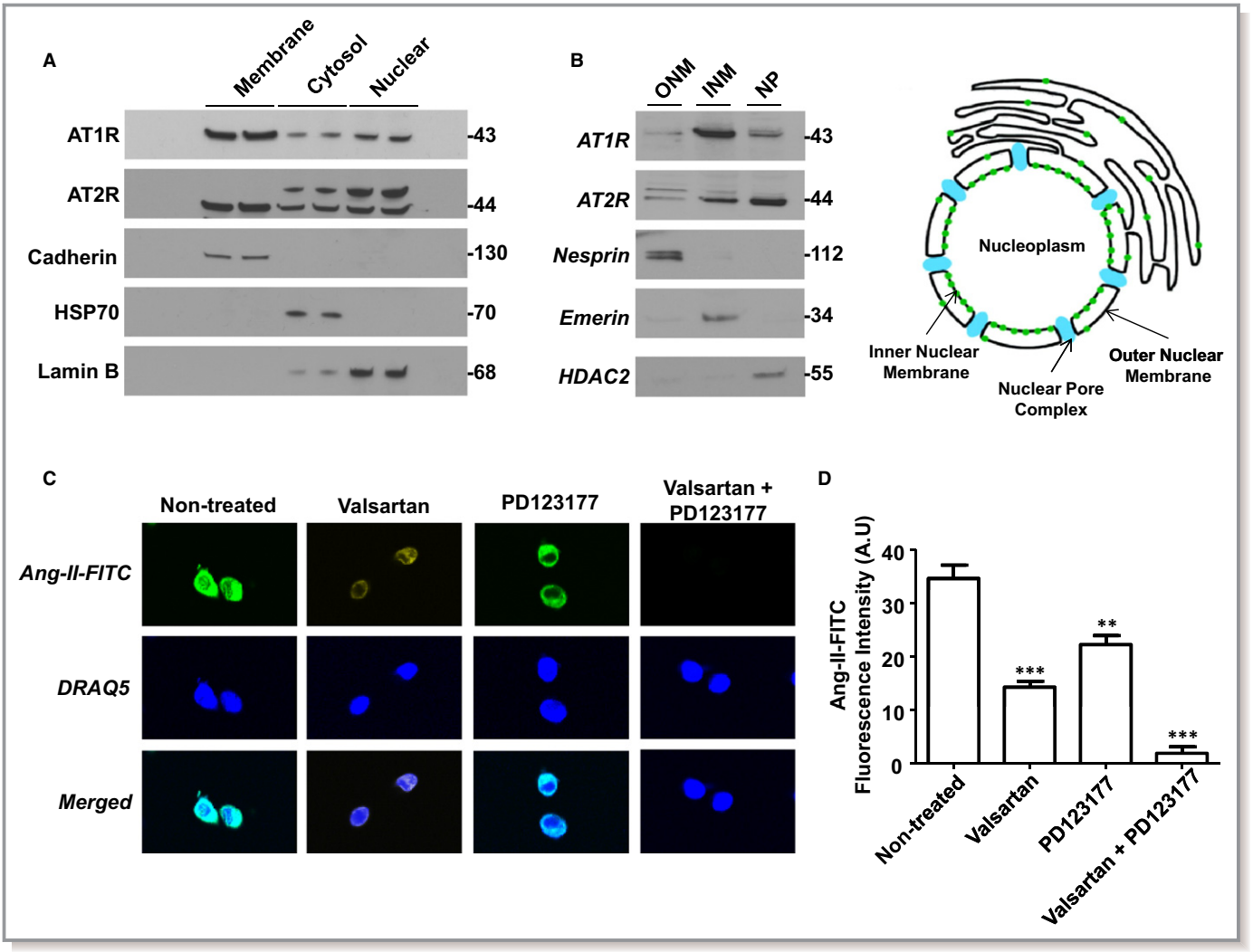

Figure 1. Endogenous AT1Rs and AT2Rs localize to the nucleus in canine atrial fibroblasts. A, Cultured fibroblasts were fractionated by differential centrifugation and the purity of membrane, cytosolic, and nuclear fractions (50 μg) were validated by immunoblotting for pan-cadherin, HSP70, and lamin B (n=5 separate experiments). The presence of AT1Rs and AT2Rs was determined by immunoblotting. The positions of molecular weight markers are indicated at the right (in kDa). B, Subfractionation of isolated fibroblast nuclei was performed to separate outer (ONM) and inner (INM) nuclear membranes and nucleoplasm (NP). Nesprin, emerin, and HDAC2 served as markers of the ONM, INM/lamina and nucleoplasm, respectively. Immunoblotting detected AT1Rs and AT2Rs in nuclear subfractions. The positions of molecular weight markers are indicated at the right (in kDa). C, Isolated nuclei were plated on laminin-coated 18 mm coverslips and then incubated with 100 nmol/L FITC-Ang-II at room temperature or preincubated with valsartan (1 μmol/L) and/or PD123177 (1 μmol/L) for 30 minutes prior to the addition of FITC-Ang-II. Nuclei were washed and stained with fluorescent DNA dye DRAQ5. Images were acquired with an Olympus FluoView FV1000 confocal microscope. D, Quantification of bound FITC-Ang-II fluorescence, mean±SEM. $^{**}P<0.01$, $^{***}P<0.001$, by 1-way ANOVA with Bonferroni-adjusted *t* test. N=5/condition. Ang-II indicates angiotensin-II; AT1Rs, Ang-II type 1 receptors; FITC, fluorescein isothiocyanate; HDAC2, histone deacetylase-2; INM, inner nuclear membrane; ONM, outer nuclear membrane.

with [α^{32}P]UTP to measure de novo RNA synthesis. Ang-II produced a dose-dependent increase in transcription initiation, which reached statistical significance at 10 nmol/L (Figure 4A). Both AT1R and AT2R antagonists significantly reduced transcription induced by 100-nmol/L Ang-II (Ang-II alone: 420±41 cpm/ng DNA, Ang-II+valsartan: 110.5±14 cpm/ng DNA, Ang-II+PD 123,177: 220±21 cpm/ng DNA, N=4/group, $P<0.001$). The RNA polymerase II inhibitor α-amanitin (5 μg/mL) markedly suppressed the ability of Ang-II to increase transcription initiation in isolated nuclei (Figure 4B).

To determine the mechanisms whereby activating AT1Rs or AT2Rs leads to changes in gene expression, nuclei were preincubated with an NO-selective fluorescence dye, 4,5-diaminofluorescein (DAF-2), and then exposed to Ang-II. Ang-II (100 nmol/L) elicited a statistically significant ($P<0.001$) over 6-fold increase in DAF-2 fluorescence (Figure 4C), which was abolished by the AT2R inhibitor PD 123,177 (1 μmol/L) but not significantly affected by valsartan (1 μmol/L). The Ang-II-mediated augmentation in NO-production was also eliminated when nuclei were pretreated with the NOS inhibitor L-NAME

Downloaded from http://jaha.ahajournals.org/ by guest on July 17, 2017

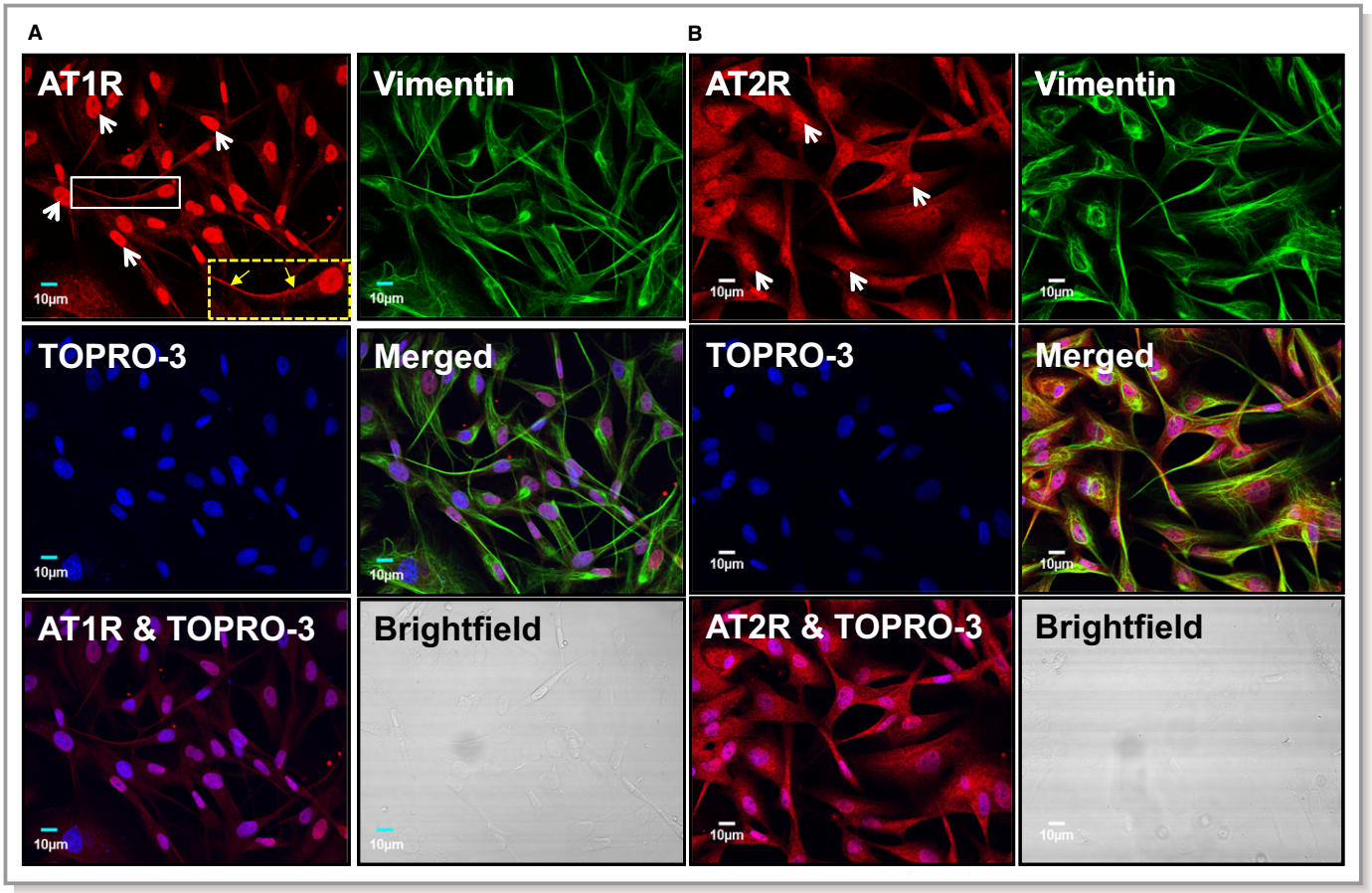

Figure 2. AT1Rs and AT2Rs colocalize with TOPRO-3 nucleic-acid stain in canine atrial fibroblasts. A, Cultured atrial fibroblasts were permeabilized and then labeled with an AT1R antibody conjugated with Alexa Fluor 488 (red), anti-vimentin conjugated with Alexa Fluor 555 (green), and TOPRO-3 (blue). Merged images indicate the extent of colocalization. The dashed box at the lower right corner of the AT1R-stained image shows an enlarged version of the fibroblast in the smaller white box. Linear membrane staining is indicated by the yellow arrows. B, Cultured atrial fibroblasts were permeabilized and then labeled with an AT2R antibody conjugated with Alexa Fluor 488 (red), anti-vimentin conjugated with Alexa Fluor 555 (green), and TOPRO-3 (blue). Merged images indicate the extent of colocalization. Brightfield images confirm the absence of cardiomyocytes from the fibroblast preparation. Similar observations were obtained from 5 different canine heart preparations for both AT1Rs and AT2Rs. AT1Rs indicates Ang-II type 1 receptors.

(1 mmol/L). Immunoblotting subsequently revealed the presence of endothelial NOS immunoreactivity in the nuclear fraction (Figure 4D).

We have previously demonstrated that cardiomyocyte nuclear AT1Rs are coupled to IP3R activation to increase nuclear Ca^{2+} concentration $[Ca^{2+}]_n$ that, in turn, plays a key role in regulating gene expression. To determine whether this pathway also functions in fibroblast nuclei, we pretreated cardiac fibroblast nuclei with a specific AT1R agonist (L-162313, 1 μmol/L) or AT2R agonist (CGP 42112A, 1 μmol/L), in the presence or absence of the IP3R blocker 2-APB (100 μmol/L) or L-NAME (1 mmol/L), and assessed transcription initiation using [α^{32}P]UTP incorporation. The results showed that the ability of AT1Rs to increase transcription initiation was reduced significantly by 2-APB and not L-NAME, whereas that of AT2R was reduced by L-NAME and not by 2-APB (Figure 4E). These results indicate that nuclear AT1Rs and AT2Rs regulate transcription via different signaling pathways.

Based on the ability of 2-APB to block the transcriptional response to nuclear AT1R activation, we examined directly the ability of Ang-II to modulate nuclear Ca^{2+} in intact atrial fibroblasts. A photolabile cell-permeable caged Ang-II (cAng-II) analog ([Tyr(DMNB)^4]Ang-II) was used to release Ang-II intracellularly, while monitoring changes in nucleoplasmic $[Ca^{2+}]$ ($[Ca^{2+}]_n$) with the membrane-permeable fluorescent Ca^{2+} indicator Fluo-4 AM. In contrast to control cells exposed to a flash of UV light, UV irradiation of cAng-II (100 nmol/L)–loaded fibroblasts generated a transient increase in nuclear fluorescence (white arrows indicate UV-irradiated cells, Figure 5A). Extracellularly administered Ang-II increased $[Ca^{2+}]_n$, albeit to a lesser extent than cAng-II (Figure 5A through 5C). The addition of poorly membrane-permeable valsartan (1 μmol/L) in the extracellular medium

Downloaded from http://jaha.ahajournals.org/ by guest on July 17, 2017

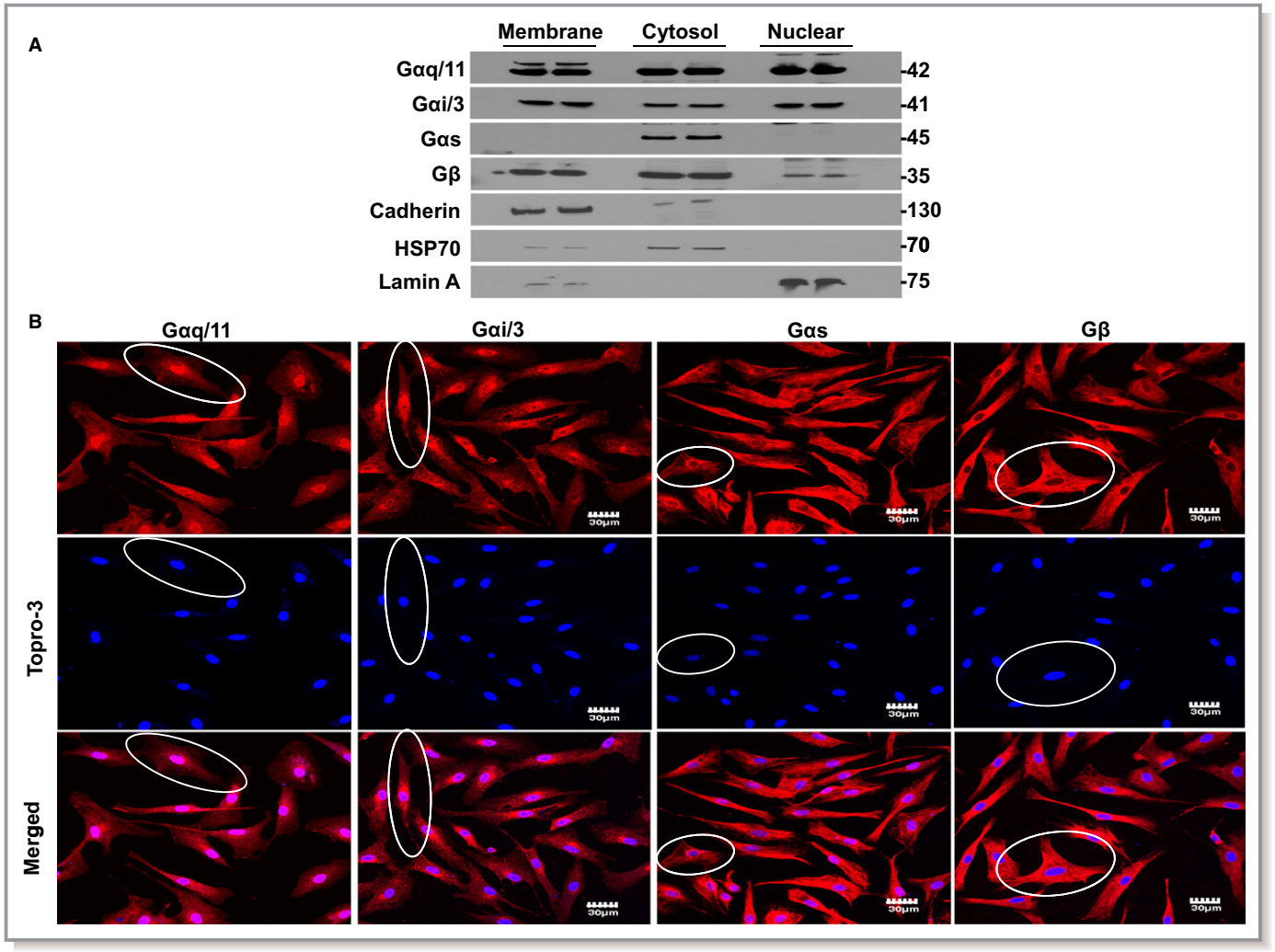

Figure 3. Presence of G protein subunits in fibroblast nuclei. A, Detection of Gαq/11, Gαi/3, Gαs, and Gβ in membrane, cytosolic, and nuclear fractions by immunoblot. Similar observations were obtained in fibroblasts isolated from each of 4 different dog hearts. The positions of molecular weight markers are indicated at the right (in kDa). B, Representative confocal images demonstrating the distribution of Gαq/11, Gαi/3, Gαs, and Gβ in permeabilized atrial fibroblasts. Superimposed confocal image showing the colocalization of G protein subunits with TOPRO-3 double-stranded DNA stain. The ovals outline illustrative cells. Gαq/11 and Gαi/3 protein staining (red) is clearly localized over the nucleus. Gαs and Gβ have much more diffuse distribution over the cell bodies, with some apparent perinuclear localization. Similar observations were obtained from 4 different canine heart preparations.

failed to affect the ability of cAng-II to increase $[Ca^{2+}]_n$, suggesting that the photolysed Ang-II actions are mediated exclusively by intracellular receptors, rather than diffusion out of cells to act via plasma-membrane ATRs. The Ang-II-induced increases in $[Ca^{2+}]_n$ were attenuated by an IP3R inhibitor, 2-APB.

The inhibitory actions of 2-APB are not specific for IP3Rs, so we employed a molecular approach to knock down IP3Rs and thereby obtain clearer information as to whether IP3Rs constitute the Ca^{2+}-release mechanism coupled to nuclear Ang-II receptor activation in atrial fibroblasts. Analysis by quantitative polymerase chain reaction suggested significant expression of IP3R type 1, 2, and 3 genes (*ITPR1*, *2*, and *3*, respectively) in fibroblasts, with *ITPR3* mRNA being the most abundant (Figure 5D). Analysis of IP3R isoform immunoreactivity in subnuclear fractions showed abundant IP3R3 in the INM and weaker immunoreactivity in the outer nuclear membrane (Figure S2), with much fainter expression of the other isoforms. We then generated siRNA constructs targeted to the mRNA for each *ITPR* isoform, along with a scrambled construct (Scr siRNA), and transfected them into fibroblasts with Lipofectamine. Figure S3 shows that each siRNA strongly suppressed mRNA expression of its target (by >80% for each), whereas Figure S4 shows substantial siRNA-induced reductions in IP3R isoform immunoreactivity. All siRNAs demonstrated some degree of cross-reactivity, with decreases in off-target mRNAs varying from about 15% to 50% in other *IP3R* subtype mRNAs. The Scr siRNA did not affect

Downloaded from http://jaha.ahajournals.org/ by guest on July 17, 2017

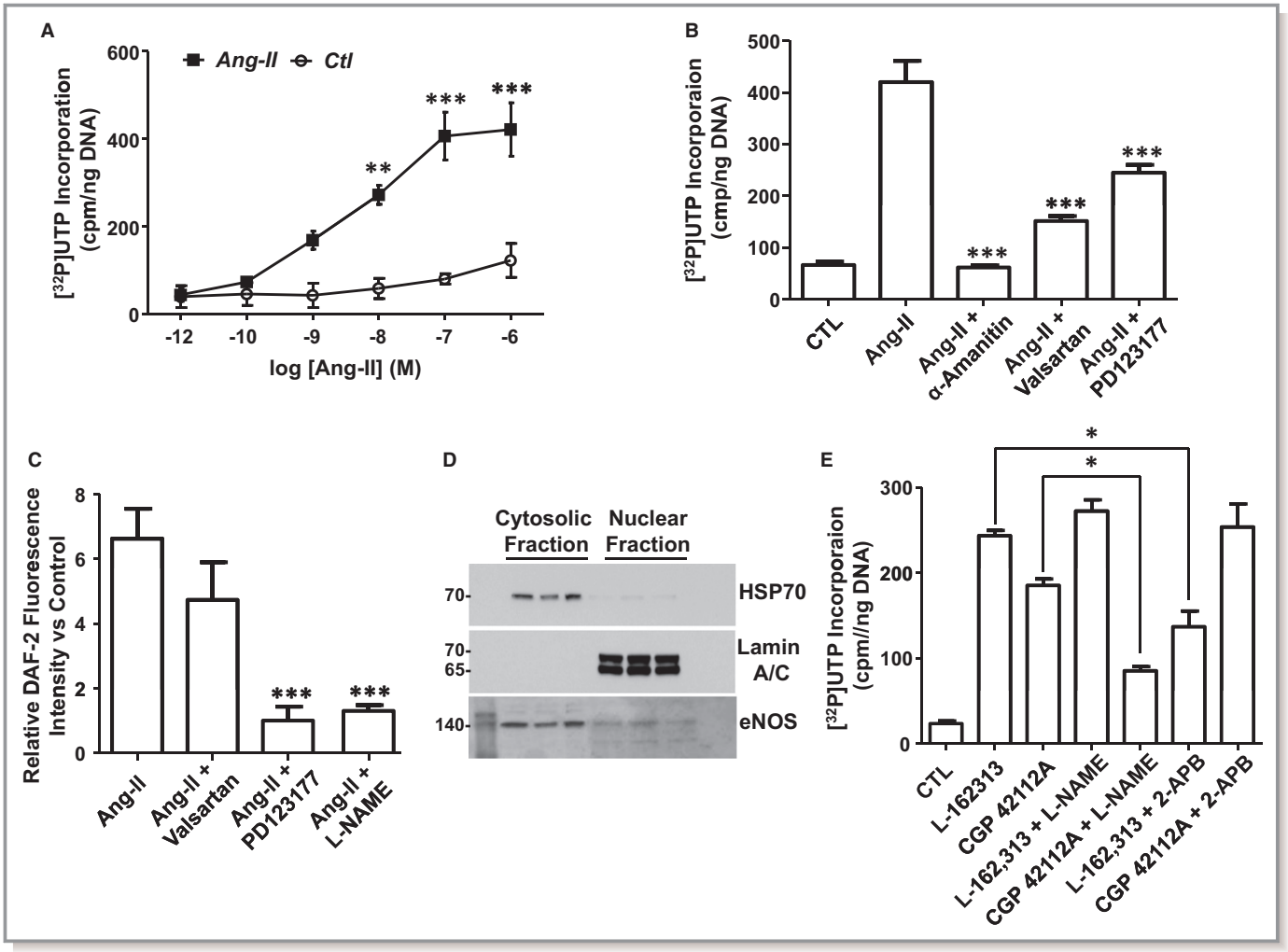

Figure 4. Nuclear AT1Rs and AT2Rs regulate RNA synthesis in isolated atrial fibroblast nuclei; IP3R and NO are underlying mediators. A, Transcription initiation was measured as [α^{32}P]UTP incorporation in nuclei treated with increasing concentrations of angiotensin-II (Ang-II). $^{**}P<0.01$, $^{***}P<0.001$, by 1-way ANOVA with Bonferroni-adjusted *t* test vs control (CTL). B, [α^{32}P]UTP incorporation was measured in nuclei treated with Ang-II (100 nmol/L) alone, or pretreated with α-amanitin (5 μg/mL), valsartan (1 μmol/L), or PD123177 (1 μmol/L) and then stimulated with Ang-II. $^{***}P<0.001$, by 1-way ANOVA with Bonferroni-adjusted *t* test vs Ang-II. C, NO production was determined by DAF-2 fluorescence in nuclei stimulated with Ang-II (100 nmol/L) alone, or pretreated with valsartan (1 μmol/L), PD123177 (1 μmol/L), or L-NAME (1 mmol/L) and then stimulated with Ang-II. Data represent mean±SEM of at least 4 separate experiments performed in triplicate and normalized to control. $^{***}P<0.001$ vs control. D, Immunoblotting for eNOS in cytosolic and nuclear enriched fractions. The positions of molecular weight markers are indicated at the left (in kDa). E, [α^{32}P]UTP incorporation measured in fibroblast nuclei treated with L-162313 (AT1R-selective agonist, 1 μmol/L) or CGP 42112A (AT2R-selective agonist, 1 μmol/L), alone or in combination with either L-NAME (1 mmol/L) or 2-APB (100 μmol/L). $^{*}P<0.05$ by 1-way ANOVA with Bonferroni-adjusted *t* test for comparisons shown. All results are mean±SEM. AT1Rs indicates Ang-II type 1 receptors; 2-APB, 2-aminoethoxydiphenyl borate; DAF-2, 4,5-diaminofluorescein; eNOS, endothelial nitric oxide synthase; L-NAME, N(G)-nitro-L-arginine methyl ester.

the abundance of *ITPR2* or *3* mRNA, and was associated with a small (under 20%) decrease in that of *ITPR1*. Figure 5E shows the effect of knocking down each *ITPR* subtype on the ability of intracellular photolysis of cAng-II to evoke a change in nuclear Fluo4 fluorescence. *ITPR3* siRNA virtually abolished the ability of intracellular release of Ang-II to increase nuclear Ca^{2+}, whereas *ITPR2* siRNA reduced it significantly (by about 40%). Knocking down *ITPR1* did not produce a statistically significant effect. The combination of all 3 *ITPR* siRNAs completely suppressed the ability of cAng-II uncaging to increase nuclear Fluo4 fluorescence (Figure 5B and 5C). These results indicate that nuclear ATR-activation increases $[Ca^{2+}]_n$ via IP3Rs, principally IP3R3.

Intracellular Ang-II Regulates Fibroblast Proliferation

Having demonstrated that nuclear ATRs are coupled to effectors, we moved to study their potential functional relevance. We first assessed effects on the proliferative

Downloaded from http://jaha.ahajournals.org/ by guest on July 17, 2017

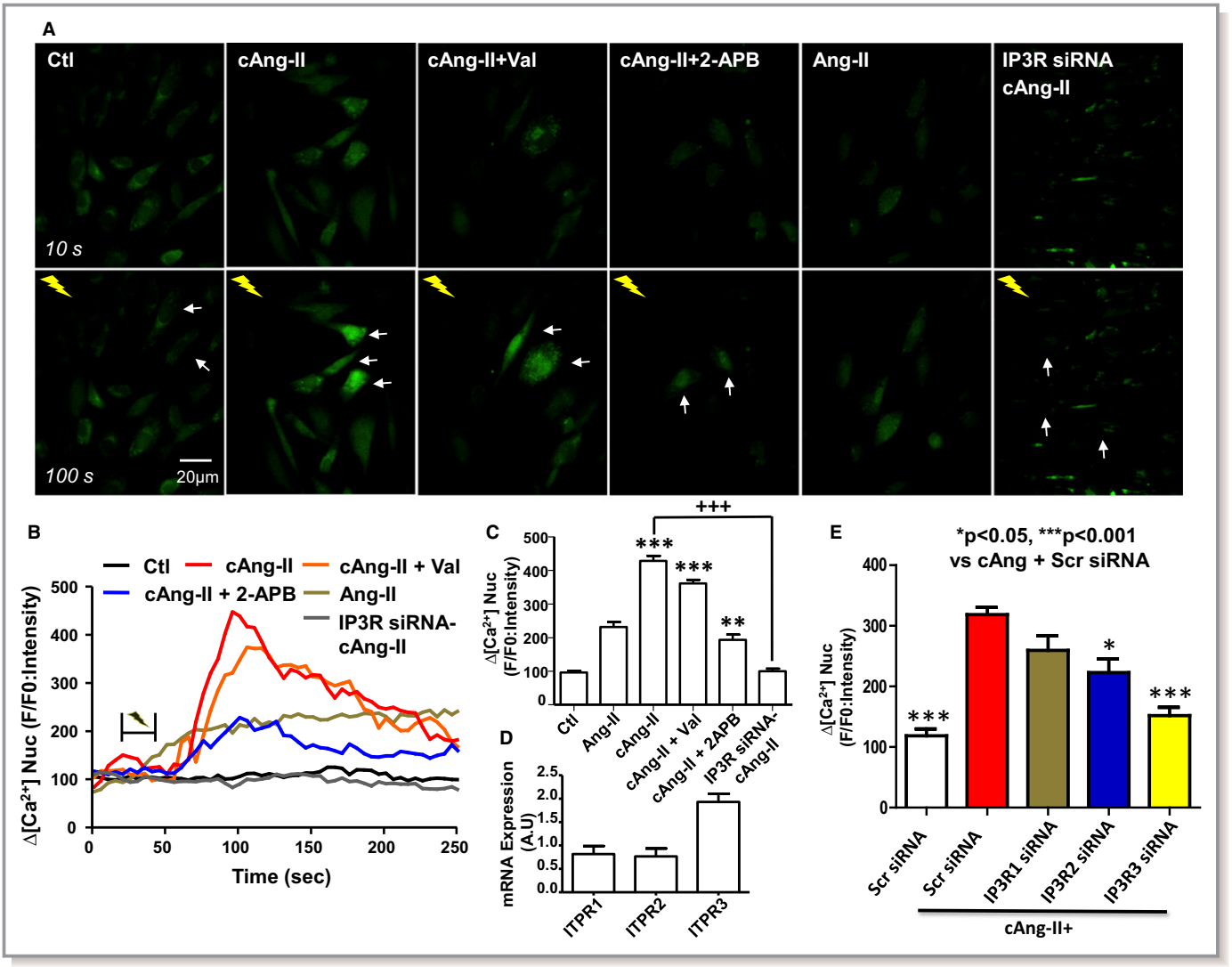

Figure 5. Intracellular Ang-II regulates nuclear Ca^{2+}. A, Cultured atrial fibroblasts were seeded on FluoroDish culture dishes and changes in $[Ca^{2+}]_n$ were followed with Fluo4-AM, a cell-permeable fluorescent calcium indicator. Cells were incubated with cAng-II (100 nmol/L), caged angiotensin-II (cAng-II), and valsartan (Val) (1 μmol/L), or cAng-II and 2-APB (100 μmol/L). Where indicated, Ang-II was added directly to the extracellular media. Images shown are before (T=10 s) and after (T=100 s) flash photolysis. White arrows indicate the cells targeted with UV light (note: cells treated with external Ang-II were not irradiated). B, Representative recordings of changes in $[Ca^{2+}]_n$. C, Fluorescence signals, presented as background-subtracted normalized fluorescence (%F/F_0), where F is the fluorescence intensity, and F_0 is the resting fluorescence recorded in the same fibroblast under steady-state conditions prior to photolysis. $^{**}P<0.01$, $^{***}P<0.001$ by 1-way ANOVA with Bonferroni-adjusted *t* test vs control (Ctl). $^{+++}P<0.001$ by 1-way ANOVA with Bonferroni-adjusted *t* test vs cAng-II. D, Expression of IP3R1, IP3R2, IP3R3 as determined by qPCR. E, Fluorescence signal changes after siRNA-induced IP3R-gene silencing, presented as background-subtracted normalized fluorescence (%F/F0), where %F is the %fluorescence intensity upon photolysis of cAng-II relative to F_0 (resting fluorescence in the same fibroblast prior to photolysis). $^{*}P<0.05$, $^{***}P<0.001$ by 1-way ANOVA with Bonferroni-adjusted *t* test vs cAng+Scr siRNA. The white bar shows the control results obtained without infusion of cAng-II; colored bars are results in the presence of cAng-II. Scr siRNA, scrambled control; 2-APB indicates available pharmacological probe 2-aminoethoxydiphenyl borate; Ang-II, angiotensin II; cAng-II+, signals following photolysis of cAng-II; qPCR, quantitative polymerase chain reaction. All results are mean±SEM.

capacity of atrial fibroblasts originally plated at equal density. Stimulation of atrial fibroblasts with extracellular Ang-II resulted in a significant increase in [^{3}H]thymidine incorporation compared to nontreated fibroblasts (Figure 6A). Pretreatment with valsartan (AT1R blocker) and PD 123,177 (AT2R blocker) prior to the Ang-II treatment prevented the increase in [^{3}H]thymidine incorporation. Synchronized fibroblasts loaded with cAng-II were UV-irradiated and [^{3}H]thymidine uptake was measured 24 hours later. Compared to basal UV-irradiated levels, [^{3}H]thymidine uptake increased substantially (Figure 6B). Extracellular AT1R and AT2R blockers did not prevent this rise. A nonphotolysable cAng-II analog (Tyr (DMNB)^{4}Ang-II-ODMNB, scramble) did not alter [^{3}H]thymidine uptake (Figure 6B).

Downloaded from http://jaha.ahajournals.org/ by guest on July 17, 2017

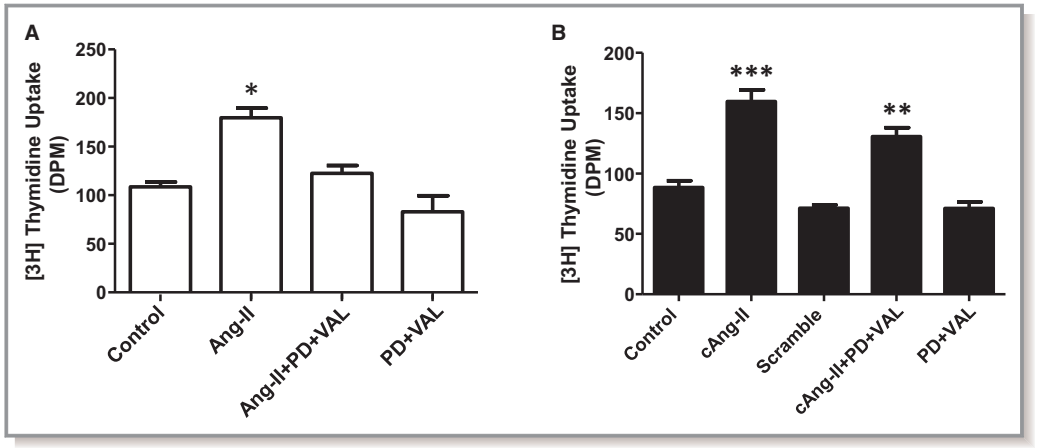

Figure 6. Intracellular Ang-II regulates fibroblast proliferation. A, [^{3}H]Thymidine incorporation in atrial fibroblasts treated in parallel with medium alone; Ang-II (100 nmol/L), alone or pretreated with PD123177 (1 μmol/L) and valsartan (1 μmol/L); and PD123177 (1 μmol/L) and valsartan (1 μmol/L) without Ang-II. B, [^{3}H]Thymidine incorporation in photolysed atrial fibroblasts treated with medium alone; cAng-II (100 nmol/L); scrambled cAng-II analog (100 nmol/L); cAng-II plus extracellular PD123177 (1 μmol/L) and valsartan (1 μmol/L); and extracellular PD123177 (1 μmol/L) and valsartan (1 μmol/L) without cAng-II. *P<0.05, **P<0.01, ***P<0.001 by 1-way ANOVA with Bonferroni-adjusted t test vs control (Ctl). N=4/group. Ang-II indicates angiotensin II; DPM, disintegrations per minute; PD, PD123177; VAL, valsartan. All results are mean±SEM.

Intracellular Ang-II Regulates Collagen Expression

We then evaluated effects on collagen synthesis in atrial fibroblasts. Growth-arrested cultures were treated with Ang-II, cAng-II, or each in combination with valsartan and PD 123,177. Collagen 1A1, 1A2, and 3A1 expression was determined at the mRNA level and collagen 1 secretion was measured by Western blot. In response to extracellular Ang-II, collagen 3A1 and 1A1 mRNA levels were increased while collagen 1A2 levels demonstrated a tendency to increase that failed to reach statistical significance (Figure 7A). Intracellular photolysis of cAng-II evoked an increase in all 3 collagen-isoform mRNAs that was not prevented by extracellular AT1R and AT2R blockers. Immunoblotting of collagen-1 secreted in the media (Figure 7B) provided results (Figure 7C) roughly paralleling those of mRNA expression, and indicate that intracellular Ang-II signaling increases collagen secretion as well as its gene expression.

Intracrine Ang-II System Changes in CHF

To evaluate potential changes in the atrial fibroblast intracellular Ang-II system in profibrotic pathology, we measured atrial fibroblast mRNA-expression of the genes encoding AT1Rs and AT2Rs (*AGTR1* and *AGTR2*, respectively) in a canine CHF model in which fibrosis is central to AF development.[11] *AGTR1* mRNA levels were significantly upregulated, whereas *AGTR2* mRNA levels did not show any statistically significant changes (Figure 8A and 8B). Intracellular Ang-II concentrations, measured by competitive ELISA, were also upregulated (control: 5.2±1.8 versus CHF: 17.9±1.4 pmol/mg protein P<0.01; Figure 8C). At the protein level, plasma membrane AT1R immunoreactivity remained unchanged in the CHF model, whereas nuclear AT1R immunoreactivity was significantly increased (Figure 8D and 8E). Consistent with the mRNA data, overall AT2R immunoreactivity, both in membrane and nuclear fractions, remained unaffected (Figure 8E). However, we observed increased abundance of a higher molecular mass band of AT2R immunoreactivity (≈52 kDa) in the nuclear fraction as quantified in Figure 8F (top). To determine whether the slower-migrating band corresponds to a glycosylated form of AT2R, we incubated the isolated membrane and nuclear fractions with peptide N-glycosidase F, which catalyzes the cleavage of N-linked oligosaccharides. Peptide N-glycosidase F digestion eliminated the higher molecular-mass AT2R bands (Figure 8F, bottom). The lower mass band that appeared in the peptide N-glycosidase F–treated group most likely represents the receptor in its totally deglycosylated form. These results suggest that in CHF the glycosylation status of nuclear AT2R has been altered, although its abundance has not been changed.

Discussion

Main Findings

In the present study we have demonstrated (1) the presence of nuclear AT1Rs and AT2Rs in atrial fibroblasts; (2) the presence of nuclear G-protein subunits; (3) the involvement of IP3Rs and NOS in the coupling, respectively, of nuclear AT1R

Downloaded from http://jaha.ahajournals.org/ by guest on July 17, 2017

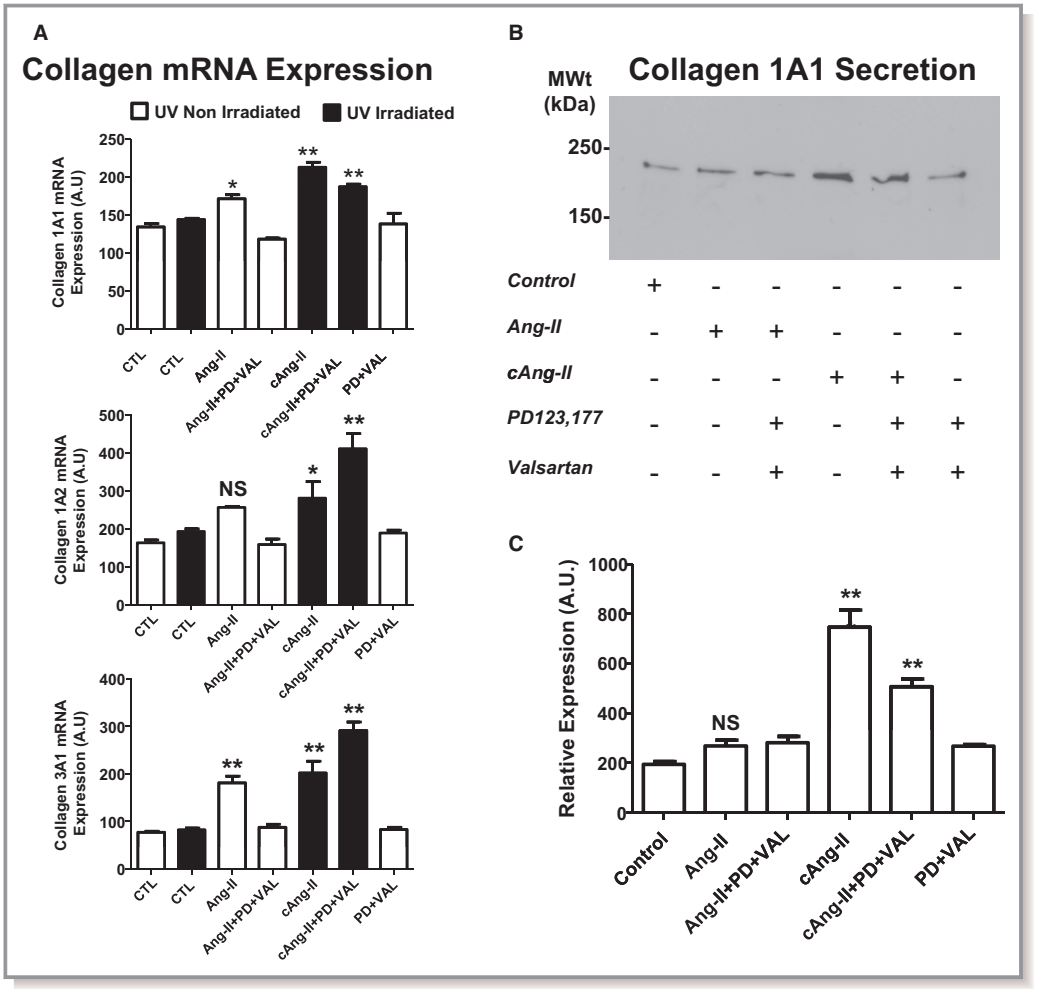

Figure 7. Intracellular Ang-II regulates collagen synthesis and secretion. A, Quantification of mRNA for collagen 1A1 (top), collagen 1A2 (middle), and collagen 3A1 (bottom) in cultured fibroblasts treated without (CTL, open bar) or with UV-irradiation (CTL, solid bar) or with AngII (100 nmol/L), Ang-II (100 nmol/L) with PD123177 (1 μmol/L) and valsartan (1 μmol/L) pretreatment, photolysis of intracellular cAng-II (100 nmol/L) without or with PD123177 (PD, 1 μmol/L) and valsartan (VAL, 1 μmol/L) pretreatment, or with PD+VAL alone. *P<0.05, **P<0.01 by 2-way ANOVA with Bonferroni-adjusted t test vs respective control (CTL); main factor effects examined: group and irradiated/nonirradiated. B, Representative immunoblots of collagen 1 in conditioned culture medium under the conditions shown. C, Quantification of collagen 1 immunoreactivity from the type of immunoblots shown in (B). Band intensities were analyzed by densitometry. **P<0.01 by 1-way ANOVA with Bonferroni-adjusted t test vs control. N=4/group, Ang-II indicates angiotensin II; NS, nonsignificant; PD, PD123177; VAL, valsartan. All results are mean±SEM.

and AT2R activation to nuclear Ca^{2+} and NO mobilization and associated transcriptional responses; (4) the regulation of IP3R-related nuclear Ca^{2+} transport by intracellular Ang-II in intact atrial fibroblasts independently of plasma membrane AT1Rs; (5) the control of fibroblast proliferation and collagen-1 secretion by intracellular Ang-II; and (6) the upregulation of intracellular Ang-II and nuclear AT1Rs, along with alterations in the glycosylation of nuclear AT2Rs, in CHF. These findings suggest that intracellular Ang-II may participate in structural remodeling by controlling fibroblast function through activation of nuclear AT1Rs and AT2Rs.

Relation to Previous Studies of Nuclear Receptors

Fibroblasts play a key role in cardiac development and arrhythmogenesis, and are fundamental in defining heart structure and function.[13–15] Although classical 7 transmembrane-domain G-protein coupled receptors (GPCRs) including ATRs,[16] endothelin receptors (ETA, ETB),[17] α-adrenergic receptors (α_1AR),[18] β-adrenergic receptors (β_1AR, β_3AR),[19] and urotensin receptors[20] have been reported on cardiac nuclear membranes, to our knowledge nothing is known about the

Downloaded from http://jaha.ahajournals.org/ by guest on July 17, 2017

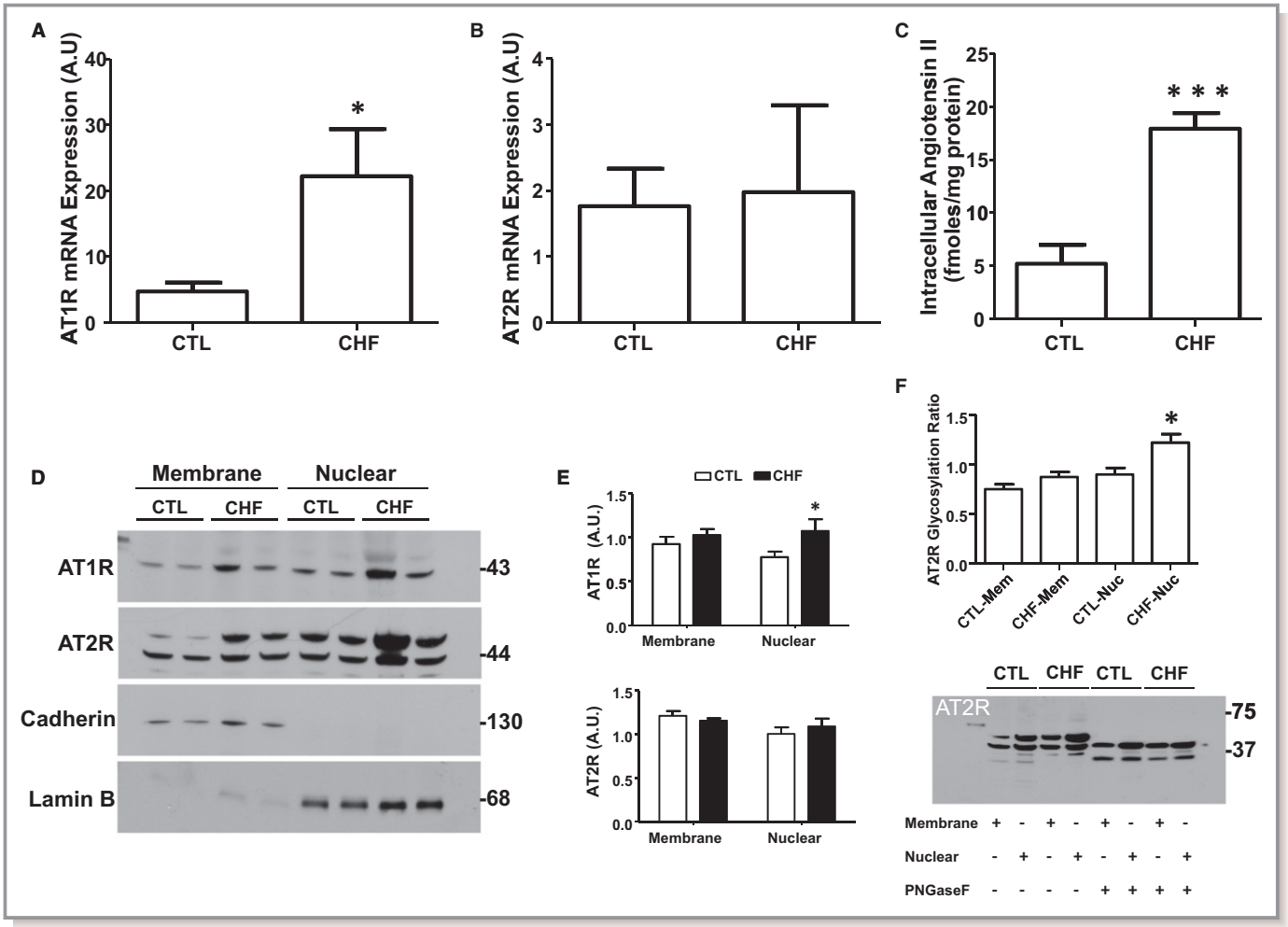

Figure 8. Congestive heart failure (CHF) affects atrial fibroblast intracellular Ang-II signaling components. A, Expression of AT1R and (B) AT2R mRNA in freshly isolated canine atrial fibroblasts. C, Intracellular Ang-II concentrations in isolated fibroblasts. D, Immunoblotting for AT1Rs, AT2Rs, pan-cadherin, and lamin-B in membrane and nuclear proteins from freshly isolated CTL and 2-week VTP fibroblasts. The positions of molecular weight markers are indicated at the right (in kDa). E, Quantification (mean±SEM) of AT1R and AT2R immunoreactivity in membrane and nuclear fractions normalized to, respectively, pan-cadherin and lamin-B. Note that for AT2R, the results shown are for the nonglycosylated band. An analysis of AT2R glycosylation is shown in (F). F, Peptide N-glycosidase F (PNGase F) effects on nuclear AT2R immunoblots. Nuclei were incubated with PNGase F at 37°C for 7.5 hours followed by immunoblotting for AT2R. Glycosylation Ratio was calculated using non-PNGase F-treated samples by dividing the intensity of the glycosylated band by that of the nonglycosylated band. The positions of molecular weight markers are indicated at the right (in kDa). **P*<0.05, ****P*<0.001, by nonpaired *t* test, CTL vs CHF; N=3 to 4 dogs/group. Ang-II indicates angiotensin-II; AT1R, Ang-II type 1 receptor; CTL, control; VTP, ventricular tachypacing. All results are mean±SEM.

specific presence or role of nuclear GPCRs in cardiac fibroblasts. The prior work on cardiac nuclear GPCRs was achieved with cardiac myocytes or total cardiac nuclear preparations from dissected cardiac issue, and hence could not identify a contribution of noncardiomyocyte nuclear GPCRs. The presence of both AT1Rs and AT2Rs has been demonstrated in adult human atrial fibroblasts,[21,22] dermal fibroblasts, synovial fibroblasts, and lung fibroblasts.[23] AT1Rs are upregulated, whereas AT2Rs remain unchanged, in left-atrial tissue samples obtained from patients with atrial fibrillation.[24] None of these earlier studies examined nuclear-localized ATRs in fibroblasts. Thus, to our knowledge, this is the first report demonstrating the presence of subcellular Ang-II binding sites within isolated canine atrial fibroblasts and more precisely the presence of AT1Rs and AT2Rs on the inner lipid bilayer of the nuclear envelope. Putative nuclear-localization sequences have been identified in both AT1Rs and AT2Rs.[25] Trafficking to the INM may occur following biosynthesis through a vesicle-mediated pathway, nuclear pore complex–dependent and -independent pathways and via diffusion–retention.[26] Our finding of post-translational modifications in nuclear AT2Rs with CHF is consistent with previous reports that described 5 glycosylation sites in the extracellular N-terminal domain of AT2Rs.[27] The glycosylated AT2Rs in the nucleus likely reflect

Downloaded from http://jaha.ahajournals.org/ by guest on July 17, 2017

posttranslational modification in the Golgi apparatus followed by trafficking to the nucleus.[28]

Nuclear ATR-Effector Coupling in Fibroblasts

Heterotrimeric G proteins play a central role in GPCR-mediated signal transduction and serve as cellular switches to control at the molecular level the functional responses to GPCR activation.[29] In the present study, Gαq/11, Gαi3, and Gβ were detected in the nuclear fraction, whereas Gαs was only found in the cytoplasm. AT1R signaling occurs principally via $G\alpha_{q11}$ and involves the production of inositol trisphosphate and mobilization of intracellular Ca^{2+}; in contrast, AT2Rs commonly signal through Gαi3 to activate the NO/cGMP pathway.[30,31] In nuclei isolated from atrial fibroblasts, AT2Rs were responsible for Ang-II-dependent NO production, since the AT1R-selective antagonist valsartan had no effect on DAF-2 fluorescence, whereas the AT2R-selective antagonist PD 123,319 reduced DAF-2 fluorescence to levels similar to those observed when nuclei were pretreated with NOS inhibitor, L-NAME. Consistent with previous findings in fibroblast nuclei isolated from whole heart, endothelial NOS immunoreactivity was detected in nuclei isolated from fibroblasts.[32] Furthermore, consistent with our previous studies of cardiomyocyte nuclei,[16,19,33,34] we observed a dose-dependent increase in de novo RNA synthesis in nuclei treated with Ang-II. We noted in the present study that the nuclear AT1R-mediated increase in transcription involves activation of IP3Rs, whereas AT2Rs increase transcription via NOS activation. IP3Rs are a family of Ca^{2+}-permeable channels comprising 3 isoforms that predominantly localize to the nuclear envelope. IP3R signaling requires the presence of phosphatidylinositol 4,5-bisphosphate, phosphatidylinositol kinases, phospholipase C, and diacylglycerol kinases: All of these are present in the nuclear membrane.[35] Using a cell-permeable photoreleasable Ang-II analog in intact fibroblasts, we demonstrated that intracellular Ang-II generates an IP3R-dependant increase in $[Ca^{2+}]_n$ that was not prevented by extracellular AT1R blockers, but was suppressed by the IP3R-blocker 2-APB or by siRNA-mediated knockdown of IP3Rs.

Potential Role of Intracellular Ang-II in Fibroblast Proliferation and Extracellular Matrix Secretion

Fibroblasts respond to a wide range of neurohormonal stimuli with proliferation and increased production and secretion of components of the extracellular matrix, leading to pathological remodeling and altered cardiac function.[1] Ang-II-induced fibroblast proliferation is mediated through autocrine/paracrine factors.[36] Here, we report a novel regulatory aspect of fibroblast physiology: intracrine Ang-II-mediated proliferation and increased collagen gene-expression and secretion. Extracellular Ang-II alone produced a significant increase in fibroblast number but not in collagen-1 gene expression and secretion, whereas intracellular photolysis of cAng-II significantly increased both fibroblast proliferation and collagen secretion. In intact fibroblasts, the effects of increased intracellular Ang-II were not prevented by the presence of valsartan and PD 123,177 in the extracellular media, indicating that the effects of intracellular Ang-II were not mediated by receptors at the cell surface.

Novelty and Potential Significance

To our knowledge, our study is the first demonstration in the literature of nuclear localization and function of G-coupled protein receptors in fibroblasts. In addition, we found that a pathological cardiac condition, heart failure, in which angiotensin-signaling and associated tissue fibrosis are prominent,[4] causes remodeling of the intracellular/nuclear-receptor Ang-II system. Specifically, we noted an increase in atrial-fibroblast intracellular Ang-II concentration and nuclear AT1R expression, as well as altered glycosylation of nuclear AT2Rs, in an experimental model of CHF in which atrial fibrosis is centrally involved in AF promotion.[37] Atrial fibrosis is an extremely common feature believed to be of pathophysiological significance in clinical AF,[3] and has recently been termed "the hallmark of the arrhythmogenic substrate in AF."[38] Inhibition of Ang-II production by angiotensin-converting enzyme inhibition prevents development of the AF substrate in experimental CHF, in which AT1R expression in left-atrial tissue is increased along with plasma Ang-II concentrations.[39] In light of our observation that nuclear ATRs regulate fibroblast proliferation and collagen secretion, changes in atrial fibroblast intracellular Ang-II signaling may be of pathophysiological importance in CHF and possibly other AF-related conditions. Furthermore, while AF is the most common clinical arrhythmia and is associated with considerable morbidity and mortality, the available treatment options remain inadequate[40]; improvements in our understanding of basic underlying mechanisms are needed in order to identify potential new therapeutic targets.[41] Novel approaches to specifically block nuclear G-protein coupled receptor signaling are in development; if successful, these could provide entirely new ways to prevent development of the AF substrate.

Potential Limitations

Fibroblasts may be affected during enzymatic digestion of cardiac tissue. Fibroblasts also greatly alter their morphological and functional properties after prolonged cell culture and passage; therefore, we used fibroblasts that were either freshly isolated or cultured for short periods of no more than 3 to 4 days. In vivo, fibroblasts may be coupled to

Downloaded from http://jaha.ahajournals.org/ by guest on July 17, 2017

cardiomyocytes, either electrically or via paracrine interactions; hence, our in vitro observations should be extrapolated cautiously to the in vivo setting.[2] Mitochondrial Ang-II receptors have been described recently: thus, in our cAng-II experiments we cannot rule out the possibility of contributions from mitochondrial or other endomembrane ATRs.[42] This potential concern does not apply to our work with isolated nuclei; however, subcellular fractionation never produces complete purification and this must be considered in interpreting our findings.

Conclusions

The current study identifies a novel pathophysiological participant in cardiac profibrotic responses by demonstrating the existence of fibroblast nuclear AT1Rs and AT2Rs that are coupled to transcriptional responses through IP3R/NO pathways. Intracellular Ang-II is upregulated in CHF atrial fibroblasts, and in vitro cardiac fibroblasts exposed to increased intracellular Ang-II proliferate and secrete collagen-1. The identification and characterization of functional intracrine Ang-II signaling in atrial fibroblasts opens up new avenues of research involving the Ang-II system, with potential implications for the development of novel pharmacological interventions for the management or prevention of cardiac fibrosis and associated conditions such as AF.

Acknowledgments

The authors thank Nathalie L'Heureux and Chantal St-Cyr for outstanding technical assistance, and Jennifer Bacchi for excellent secretarial assistance with the manuscript.

Sources of Funding

This work was supported by the Canadian Institutes of Health Research and the Heart and Stroke Foundation of Canada. Tadevosyan was supported by a doctoral scholarship awarded jointly by the Fonds de la recherche en santé du Québec (FRSQ), the Réseau en santé cardiovasculaire (RSCV) and the Heart and Stroke Foundation of Québec (HSFQ).

Disclosures

None.

References

1. Souders CA, Bowers SL, Baudino TA. Cardiac fibroblast: the renaissance cell. *Circ Res*. 2009;105:1164–1176.
2. Yue L, Xie J, Nattel S. Molecular determinants of cardiac fibroblast electrical function and therapeutic implications for atrial fibrillation. *Cardiovasc Res*. 2011;89:744–753.
3. Burstein B, Nattel S. Atrial fibrosis: mechanisms and clinical relevance in atrial fibrillation. *J Am Coll Cardiol*. 2008;51:802–809.
4. Brilla CG. Renin-angiotensin-aldosterone system and myocardial fibrosis. *Cardiovasc Res*. 2000;47:1–3.
5. Brilla CG, Zhou G, Matsubara L, Weber KT. Collagen metabolism in cultured adult rat cardiac fibroblasts: response to angiotensin II and aldosterone. *J Mol Cell Cardiol*. 1994;26:809–820.
6. Tadevosyan A, Vaniotis G, Allen BG, Hebert TE, Nattel S. G protein-coupled receptor signalling in the cardiac nuclear membrane: evidence and possible roles in physiological and pathophysiological function. *J Physiol*. 2012;590:1313–1330.
7. Singh VP, Baker KM, Kumar R. Activation of the intracellular renin-angiotensin system in cardiac fibroblasts by high glucose: role in extracellular matrix production. *Am J Physiol Heart Circ Physiol*. 2008;294:H1675–H1684.
8. Singh VP, Le B, Khode R, Baker KM, Kumar R. Intracellular angiotensin II production in diabetic rats is correlated with cardiomyocyte apoptosis, oxidative stress, and cardiac fibrosis. *Diabetes*. 2008;57:3297–3306.
9. De Mello WC. Beyond the circulating renin-angiotensin aldosterone system. *Front Endocrinol (Lausanne)*. 2014;5:104.
10. Tadevosyan A, Allen BG, Nattel S. Isolation and study of cardiac nuclei from canine myocardium and adult ventricular myocytes. *Methods Mol Biol*. 2015;1234:69–80.
11. Tadevosyan A, Villeneuve LR, Fournier A, Chatenet D, Nattel S, Allen BG. Caged ligands to study the role of intracellular GPCRs. *Methods*. 2016;92:72–77.
12. Tadevosyan A, Letourneau M, Folch B, Doucet N, Villeneuve LR, Mamarbachi AM, Petrin D, Hebert TE, Fournier A, Chatenet D, Allen BG, Nattel S. Photoreleasable ligands to study intracrine angiotensin II signalling. *J Physiol*. 2015;593:521–539.
13. Burstein B, Qi XY, Yeh YH, Calderone A, Nattel S. Atrial cardiomyocyte tachycardia alters cardiac fibroblast function: a novel consideration in atrial remodeling. *Cardiovasc Res*. 2007;76:442–452.
14. Aguilar M, Qi XY, Huang H, Nattel S. Fibroblast electrical remodeling in heart failure and potential effects on atrial fibrillation. *Biophys J*. 2014;107:2444–2455.
15. Qi XY, Huang H, Ordog B, Luo X, Naud P, Sun Y, Wu CT, Dawson K, Tadevosyan A, Chen Y, Harada M, Dobrev D, Nattel S. Fibroblast inward-rectifier potassium current upregulation in profibrillatory atrial remodeling. *Circ Res*. 2015;116:836–845.
16. Tadevosyan A, Maguy A, Villeneuve LR, Babin J, Bonnefoy A, Allen BG, Nattel S. Nuclear-delimited angiotensin receptor-mediated signaling regulates cardiomyocyte gene expression. *J Biol Chem*. 2010;285:22338–22349.
17. Boivin B, Chevalier D, Villeneuve LR, Rousseau E, Allen BG. Functional endothelin receptors are present on nuclei in cardiac ventricular myocytes. *J Biol Chem*. 2003;278:29153–29163.
18. Wright CD, Chen Q, Baye NL, Huang Y, Healy CL, Kasinathan S, O'Connell TD. Nuclear alpha1-adrenergic receptors signal activated ERK localization to caveolae in adult cardiac myocytes. *Circ Res*. 2008;103:992–1000.
19. Boivin B, Lavoie C, Vaniotis G, Baragli A, Villeneuve LR, Ethier N, Trieu P, Allen BG, Hebert TE. Functional beta-adrenergic receptor signalling on nuclear membranes in adult rat and mouse ventricular cardiomyocytes. *Cardiovasc Res*. 2006;71:69–78.
20. Doan ND, Nguyen TT, Letourneau M, Turcotte K, Fournier A, Chatenet D. Biochemical and pharmacological characterization of nuclear urotensin-II binding sites in rat heart. *Br J Pharmacol*. 2012;166:243–257.
21. Brink M, Erne P, de Gasparo M, Rogg H, Schmid A, Stulz P, Bullock G. Localization of the angiotensin II receptor subtypes in the human atrium. *J Mol Cell Cardiol*. 1996;28:1789–1799.
22. Tsutsumi Y, Matsubara H, Ohkubo N, Mori Y, Nozawa Y, Murasawa S, Kijima K, Maruyama K, Masaki H, Moriguchi Y, Shibasaki Y, Kamihata H, Inada M, Iwasaka T. Angiotensin II type 2 receptor is upregulated in human heart with interstitial fibrosis, and cardiac fibroblasts are the major cell type for its expression. *Circ Res*. 1998;83:1035–1046.
23. Galindo M, Santiago B, Palao G, Gutierrez-Canas I, Ramirez JC, Pablos JL. Coexpression of AT1 and AT2 receptors by human fibroblasts is associated with resistance to angiotensin II. *Peptides*. 2005;26:1647–1653.
24. Boldt A, Wetzel U, Weigl J, Garbade J, Lauschke J, Hindricks G, Kottkamp H, Gummert JF, Dhein S. Expression of angiotensin II receptors in human left and right atrial tissue in atrial fibrillation with and without underlying mitral valve disease. *J Am Coll Cardiol*. 2003;42:1785–1792.
25. Lee DK, Lanca AJ, Cheng R, Nguyen T, Ji XD, Gobeil F Jr, Chemtob S, George SR, O'Dowd BF. Agonist-independent nuclear localization of the apelin, angiotensin AT1, and bradykinin B2 receptors. *J Biol Chem*. 2004;279:7901–7908.
26. Katta SS, Smoyer CJ, Jaspersen SL. Destination: inner nuclear membrane. *Trends Cell Biol*. 2014;24:221–229.

Downloaded from http://jaha.ahajournals.org/ by guest on July 17, 2017

27. Carey RM, Wang ZQ, Siragy HM. Role of the angiotensin type 2 receptor in the regulation of blood pressure and renal function. *Hypertension*. 2000;35:155–163.
28. Hunyady L, Bor M, Balla T, Catt KJ. Identification of a cytoplasmic Ser-Thr-Leu motif that determines agonist-induced internalization of the AT1 angiotensin receptor. *J Biol Chem*. 1994;269:31378–31382.
29. Drake MT, Shenoy SK, Lefkowitz RJ. Trafficking of G protein-coupled receptors. *Circ Res*. 2006;99:570–582.
30. Li J, Zhao X, Li X, Lerea KM, Olson SC. Angiotensin II type 2 receptor-dependent increases in nitric oxide synthase expression in the pulmonary endothelium is mediated via a G alpha i3/Ras/Raf/MAPK pathway. *Am J Physiol Cell Physiol*. 2007;292:C2185–C2196.
31. Hunyady L, Catt KJ. Pleiotropic AT1 receptor signaling pathways mediating physiological and pathogenic actions of angiotensin II. *Mol Endocrinol*. 2006;20:953–970.
32. Gwathmey TM, Shaltout HA, Pendergrass KD, Pirro NT, Figueroa JP, Rose JC, Diz DI, Chappell MC. Nuclear angiotensin II type 2 (AT2) receptors are functionally linked to nitric oxide production. *Am J Physiol Renal Physiol*. 2009;296:F1484–F1493.
33. Vaniotis G, Gora S, Nantel A, Hebert TE, Allen BG. Examining the effects of nuclear GPCRs on gene expression using isolated nuclei. *Methods Mol Biol*. 2015;1234:185–195.
34. Vaniotis G, Del Duca D, Trieu P, Rohlicek CV, Hebert TE, Allen BG. Nuclear beta-adrenergic receptors modulate gene expression in adult rat heart. *Cell Signal*. 2011;23:89–98.
35. Cardenas C, Liberona JL, Molgo J, Colasante C, Mignery GA, Jaimovich E. Nuclear inositol 1,4,5-trisphosphate receptors regulate local Ca^{2+} transients and modulate cAMP response element binding protein phosphorylation. *J Cell Sci*. 2005;118:3131–3140.
36. Bouzegrhane F, Thibault G. Is angiotensin II a proliferative factor of cardiac fibroblasts? *Cardiovasc Res*. 2002;53:304–312.
37. Li D, Fareh S, Leung TK, Nattel S. Promotion of atrial fibrillation by heart failure in dogs: atrial remodeling of a different sort. *Circulation*. 1999;100:87–95.
38. Gal P, Marrouche NF. Magnetic resonance imaging of atrial fibrosis: redefining atrial fibrillation to a syndrome. *Eur Heart J*. 2017;38:14–19.
39. Li D, Shinagawa K, Pang L, Leung TK, Cardin S, Wang Z, Nattel S. Effects of angiotensin-converting enzyme inhibition on the development of the atrial fibrillation substrate in dogs with ventricular tachypacing-induced congestive heart failure. *Circulation*. 2001;104:2608–2614.
40. Andrade J, Khairy P, Dobrev D, Nattel S. The clinical profile and pathophysiology of atrial fibrillation: relationships among clinical features, epidemiology, and mechanisms. *Circ Res*. 2014;114:1453–1468.
41. Heijman J, Algalarrondo V, Voigt N, Melka J, Wehrens XH, Dobrev D, Nattel S. The value of basic research insights into atrial fibrillation mechanisms as a guide to therapeutic innovation: a critical analysis. *Cardiovasc Res*. 2016;109:467–479.
42. Abadir PM, Foster DB, Crow M, Cooke CA, Rucker JJ, Jain A, Smith BJ, Burks TN, Cohn RD, Fedarko NS, Carey RM, O'Rourke B, Walston JD. Identification and characterization of a functional mitochondrial angiotensin system. *Proc Natl Acad Sci USA*. 2011;108:14849–14854.

Downloaded from http://jaha.ahajournals.org/ by guest on July 17, 2017

Downloaded from http://jaha.ahajournals.org/ by guest on July 17, 2017

SUPPLEMENTAL MATERIAL

Downloaded from http://jaha.ahajournals.org/ by guest on July 17, 2017

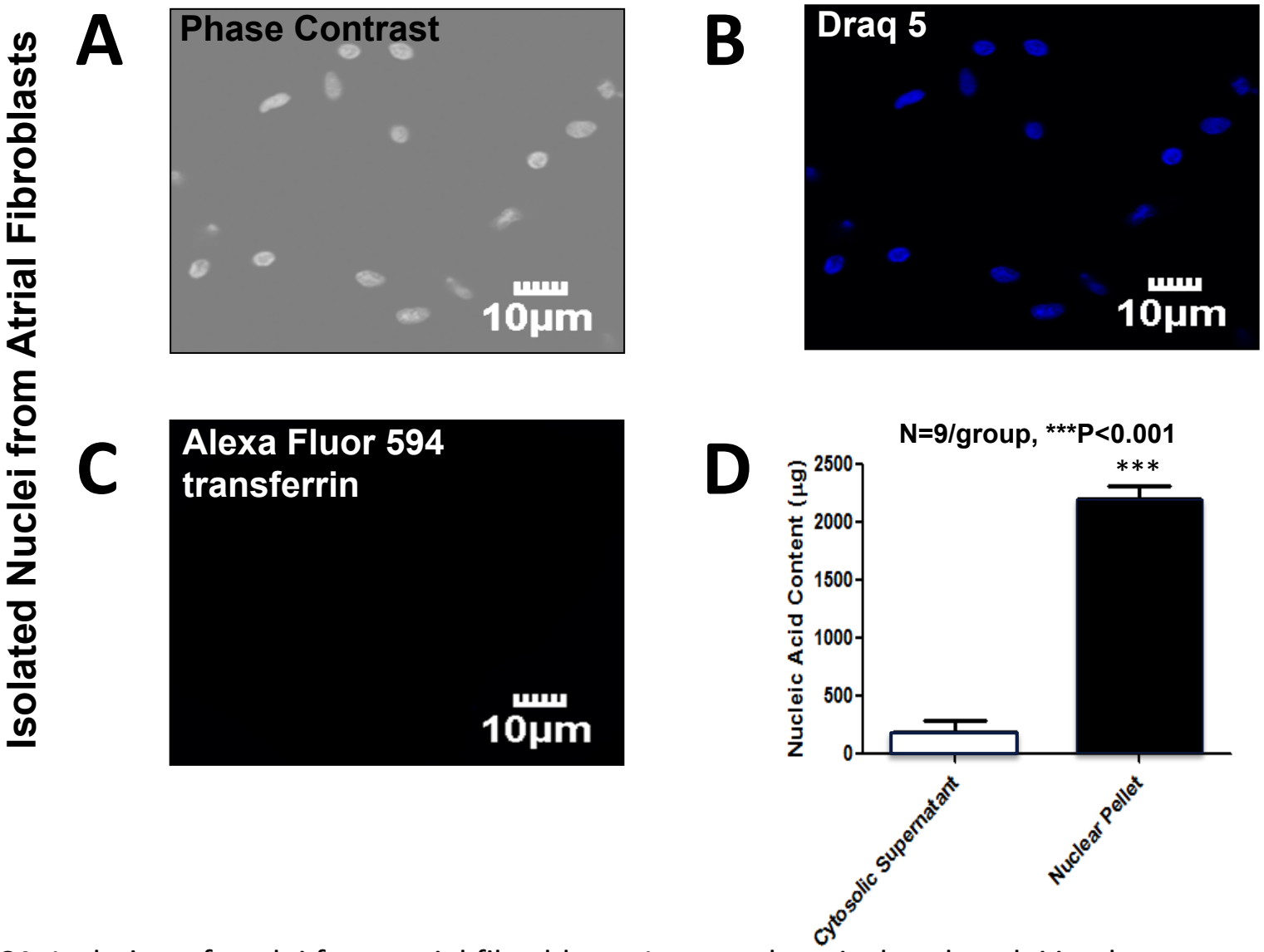

Figure S1. Isolation of nuclei from atrial fibroblasts. Images show isolated nuclei in phase contrast (**A**) or labelled with either with the DNA stain DRAQ5 (**B**) or Alexa Fluor 594-conjugated transferrin, a marker of cell surface membranes (**C**). The histogram (**D**) shows the total nucleic acid content of the cytosolic and the nuclear fractions. Mean±SEM ***P<0.001, N=9.

Downloaded from http://jaha.ahajournals.org/ by guest on July 17, 2017

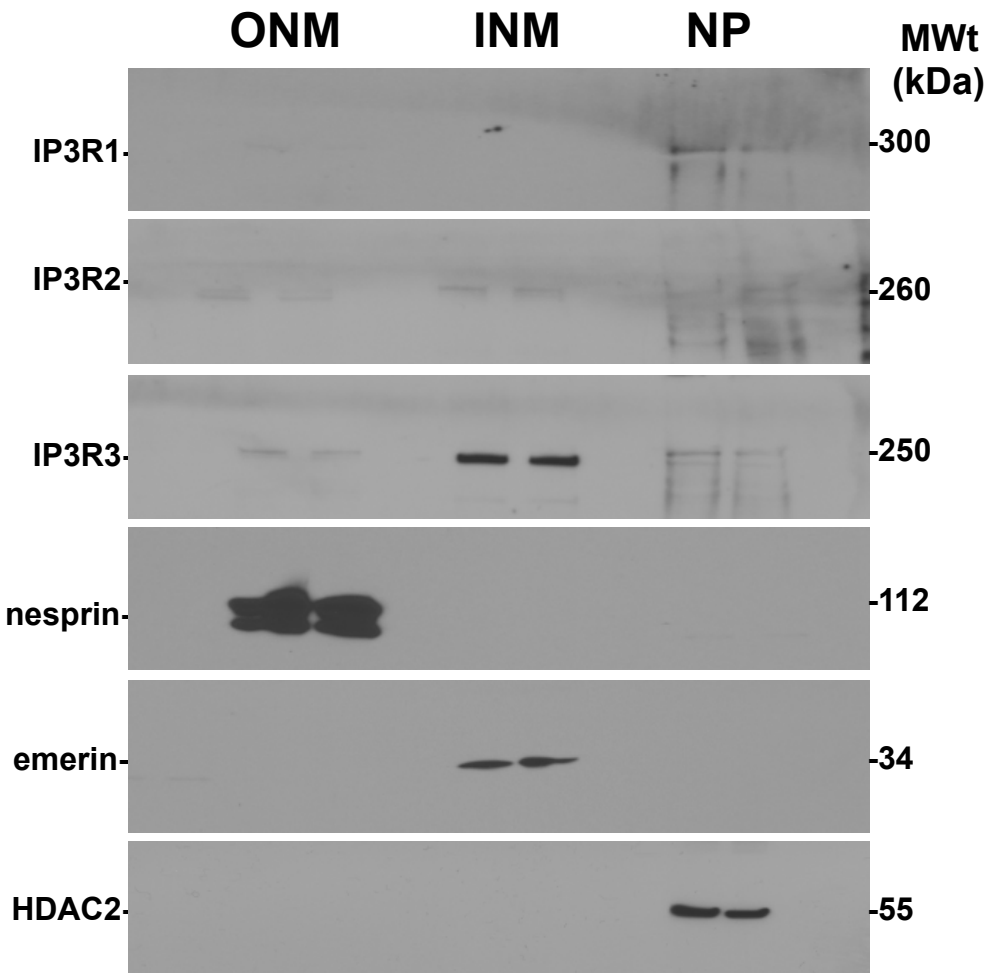

Figure S2. Detection of IP3R isoforms in fibroblast nuclei subfractions. Freshly isolated fibroblast nuclei were separated into outer nuclear membrane (ONM), inner nuclear membrane (INM), and nucleoplasm (NP) as described in Methods. Nesprin, emerin and HDAC2 immunoreactivity served as markers of the ONM, INM/lamina and NP, respectively. IP3R isoform immunoreactivity was detected in nuclear subfractions.

Downloaded from http://jaha.ahajournals.org/ by guest on July 17, 2017

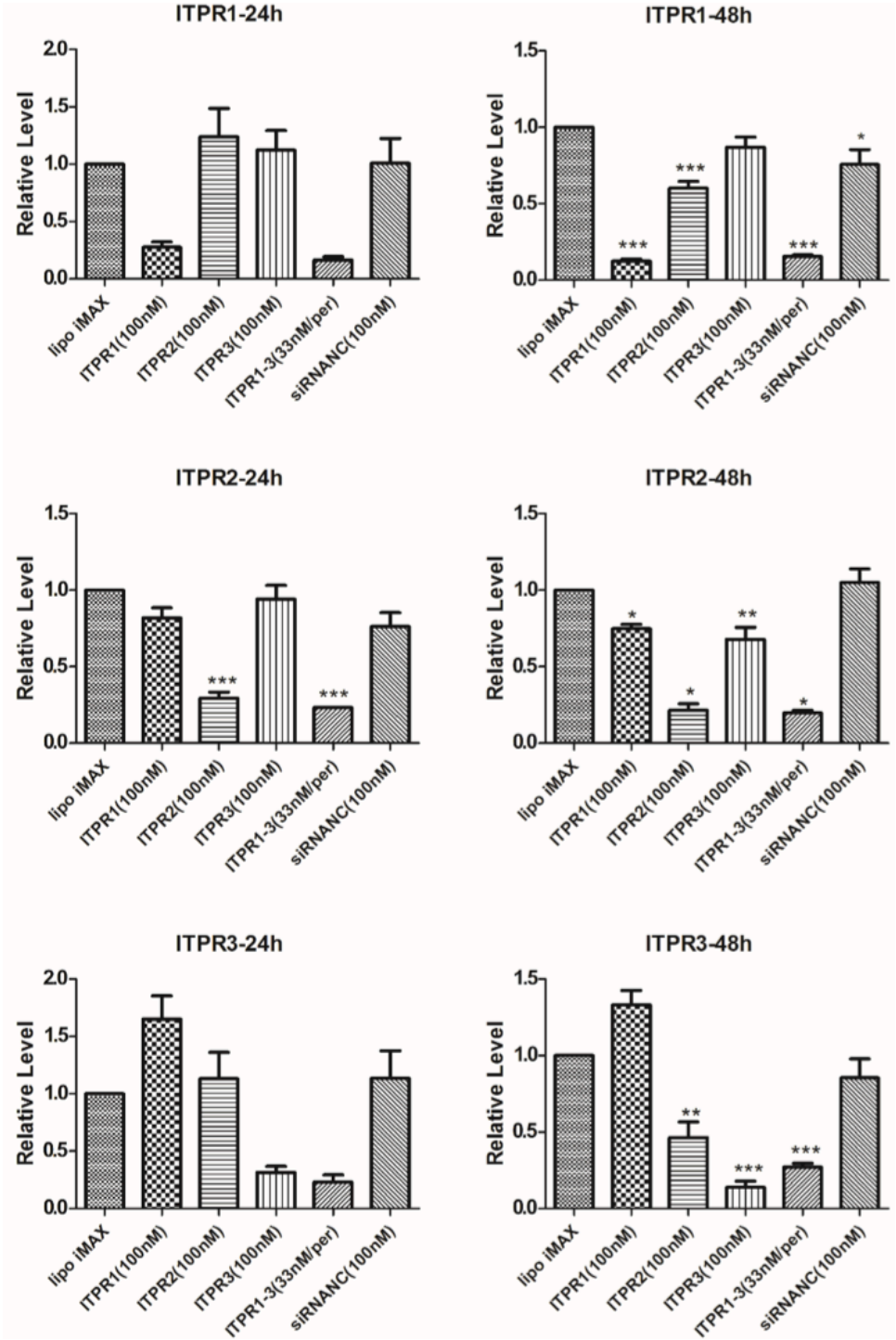

Figure S3. Efficiency of IP3R isoform knockdown by siRNA. Quantification of mRNA encoding IP3R1, IP3R2 and IP3R3 following transfection (24 and 48 hours) of cultured fibroblasts with siRNA negative control (si-NC), or siRNAs targeting the *ITPR1*, *ITPR2*, *ITPR3* or all 3 genes (si-*ITPR1*, si-*ITPR2*, si-*ITPR3*, si-*ITPR1-3* respectively) normalized to transfection with the vector alone. Mean±SEM, *P<0.05, **P<0.01, ***P<0.001 compared to vector alone.

Downloaded from http://jaha.ahajournals.org/ by guest on July 17, 2017

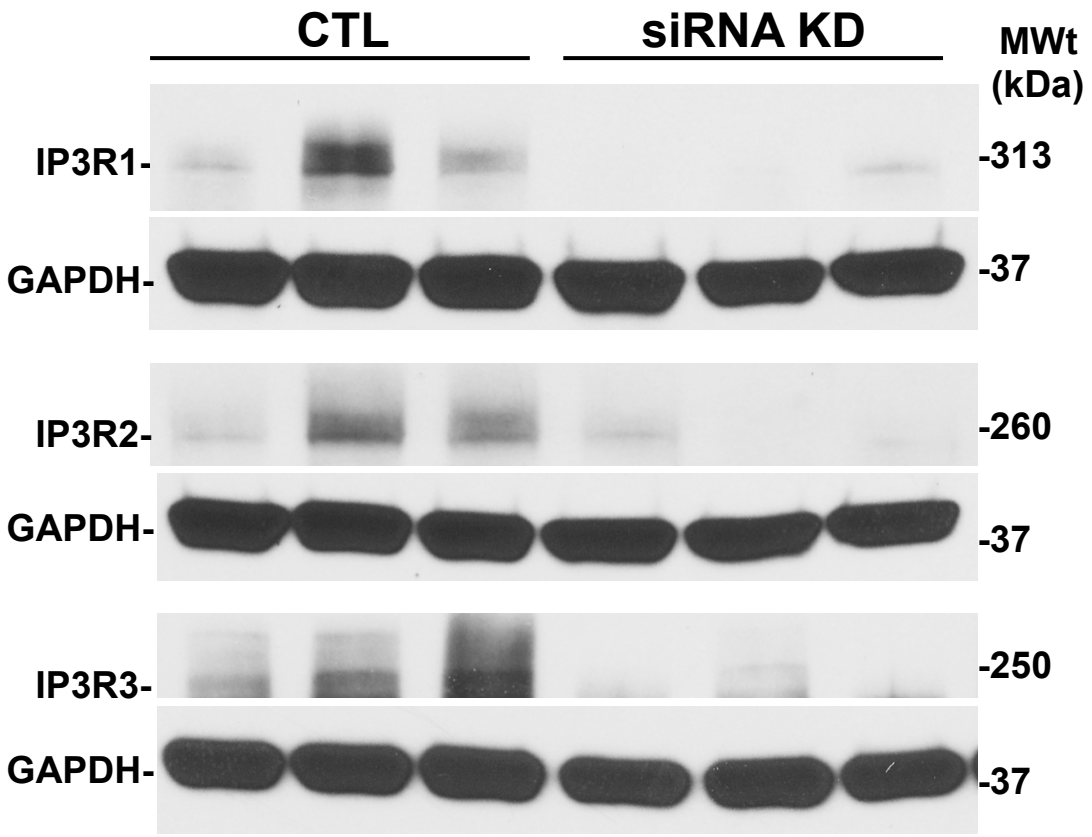

Figure S4. Validation of IP3R siRNA knockdown by immunoblotting. After 48 hours of transfection with si-*ITPR1*, si-*ITPR2* or si-*ITPR3* cells were collected, lysed and run on 7.5% Mini-PROTEAN® TGX™ Precast Protein Gels. Immunoblotting was performed using isoform specific antibodies for IP3R. GAPDH was used as a loading control.

Journal of the American Heart Association
OPEN ACCESS
American Heart Association | American Stroke Association

Intracellular Angiotensin–II Interacts With Nuclear Angiotensin Receptors in Cardiac Fibroblasts and Regulates RNA Synthesis, Cell Proliferation, and Collagen Secretion

Artavazd Tadevosyan, Jiening Xiao, Sirirat Surinkaew, Patrice Naud, Clémence Merlen, Masahide Harada, Xiaoyan Qi, David Chatenet, Alain Fournier, Bruce G. Allen and Stanley Nattel

J Am Heart Assoc. 2017;6:e004965; originally published April 5, 2017;
doi: 10.1161/JAHA.116.004965
The *Journal of the American Heart Association* is published by the American Heart Association, 7272 Greenville Avenue, Dallas, TX 75231
Online ISSN: 2047-9980

The online version of this article, along with updated information and services, is located on the World Wide Web at:
http://jaha.ahajournals.org/content/6/4/e004965

Subscriptions, Permissions, and Reprints: The *Journal of the American Heart Association* is an online only Open Access publication. Visit the Journal at http://jaha.ahajournals.org for more information.

Downloaded from http://jaha.ahajournals.org/ by guest on July 17, 2017